DOI: https://doi.org/10.24297/jap.v22i.9662

**Prototyping disruptive self-sufficiency power machines composed by cascaded power units based on thermo-hydraulic actuators**

Ramon Ferreiro Garcia (independent author)

Former, Prof. Emeritus at the University of A Coruna, Spain,

https://www.udc.es

ramon.ferreiro@udc.es

**Abstract;**

This research focuses on developing a prototype for a disruptive Self-Sustaining Power Machine (SSPM) that consists of cascaded power units (PUs). Each PU integrates thermo-mechanical and thermo-hydraulic actuators to drive hydraulic pumps connected to generators. The prototype's design leverages two thermal cycle types, sVsVs and VsVs, which enable self-sustaining operations by employing several strategic capabilities that challenge the limitations of second-kind perpetual motion machines (PMMs). Therefore, key capabilities include:

1-Performing useful mechanical work through the expansion and contraction of the Thermal Working Fluid (TWF) by adding and removing heat.

2-Utilizing recovered heat through potential superposition techniques, thereby upgrading the heat to a higher grade, which enhances heat recovery strategies.

3-Designing an efficient energy transfer chain from thermal to electrical energy via thermo-mechanical or thermo-hydraulic actuators, a hydraulic energy drive system, and conversion from hydraulic to electrical energy.

4-Configuring the system to achieve more useful work than the heat added to the initial PU downstream.

Two main prototype types are proposed to demonstrate these proposed capabilities:

1-Continuous motion using the sVsVs thermal cycle, with volumetric reservoirs for thermal working fluids (TWF) located outside the thermo-mechanical or thermo-hydraulic actuators.

2-Discontinuous motion using the VsVs thermal cycle, with volumetric reservoirs for TWF located inside the active volume of the thermo-mechanical or thermo-hydraulic actuators.

The prototypes were evaluated through case studies using air and helium as real TWFs. Results indicate that the SSPM composed of five cascaded PUs operating on an sVsVs cycle achieved a global efficiency of 149.6% (SSI of 49.6%) with helium and 126% (SSI of 26%) with air. In contrast, the VsVs cycle yielded a global efficiency of 183% (SSI of 83%) with helium and 133% (SSI of 33%) with air

**Keywords:** cascade coupling, cascade heat recovery, contraction work, expansion work, thermal potential conversion, upgrading heat recovery and vacuum work.

*Nomenclature related to thermo-hydraulic converters*

| ***Acronyms*** | ***description*** |
|---|---|
| ETWFR | External Thermal Working Fluid Reservoirs |
| HyM | Rotary Hydraulic motor-generator |
| RHyP | Reciprocating Hydraulic Mump |
| ITWFR | Internal Thermal Working Fluid Reservoirs |
| THyA | Thermal Hydraulic Actuator |
| RDAA | Reciprocating double-acting actuator (thermo-mechanic, thermo-hydraulic) |
| RDAC | Reciprocating double-acting cylinder (thermo-mechanic cylinder) |
| RDAHyR | Reciprocating double-acting hydraulic reservoirs |
| RDAHyC | Reciprocating double-acting hydraulic cylinders |
| RDAHyP | Reciprocating double-acting hydraulic pump |

*Nomenclature related to general SSPMs*

| ***Acronyms*** | ***description*** |
|---|---|
| CF | Carnot Factor |
| Cont. | contraction |
| CTF | Cooling Transfer Fluid (conventionally, thermal oil) |
| EM | electromagnetic |
| EP | Electric Power |
| Exp. | expansion |
| FCF | Forced convection fan (recirculation fan of the TWF) |
| FP | Feed pump (feed compressor of the TWF) |
| Gen | Electric Power Generator |
| HTF | Heating Transfer Fluid (conventionally, thermal il) |
| Is_eff | Isentropic efficiency (open processes) |
| LF | Losses factor (include thermo-mechanical and thermo-hydraulic losses) |
| ORC | Organic Rankine Cycle |
| PMM | Perpetual Motion Machine |
| PP | Power Plant: a group of PUs coupled in cascade |
| PU | Power Unit operating with the thermal cycle sVsVs or VsVs cycle |
| RF | Heat recovery factor (includes heat transfer losses and leaks) |
| RIT | Ratio of Isochoric low to high temperatures [$T_L/T_H$], [$T_1/T_3$] for sVsVs, and [$T_1/T_2$] for VsVs, |
| SSI | Self-Sustaining Index, which means the net free energy as % : [ $SSI = (\eta_{th} - 100)/100$ ] |
| SSHS | Self-Sustaining Heat Supply |
| SEP | Self-Electric Power: SEP ≈ SSI (net mechanical power ≈ net electrical power) |
| SKPMM | Second kind Perpetual Motion Machine |
| sp | State point of any stationary point state of a thermal cycle |
| SPPP | Self-Powered Power Plant |
| SSPM | Self-Sustaining Power Machine, Self-Sufficient Power Machine |
| SSPP | Self-Sustaining Power Plant, Self-Sufficient Power Plant |
| sVsVs | Cycle with the sequential processes: [ isentropic-adiabatic (s), Isochoric (V), s,V,s] |
| TWF | Thermal Working Fluid |
| VsVs | Cycle with the sequential processes: [ isochoric (V), isentropic-adiabatic (s), V, s] |
| ***Symbols/units*** | ***description*** |
| $p$(bar) | pressure |
| $q_i$(kJ/kg) | specific heat in to a cycle process |
| $q_{i23}$(kJ/kg) | Input heat to cycle process 2-3 |
| $q_o$(kJ/kg) | specific heat out from a cycle process |
| $q_{o41}$(kJ/kg) | output heat from cycle process 4-1 in a VsVs cycle |
| $q_{rec}$ | Recovered heat from cycle process 4-1 in a VsVs cycle |
| $Cp$(kJ/kg-K) | specific heat capacity at constant pressure |

| | |
|---|---|
| *Cv*(kJ/kg-K) | specific heat capacity at constant volume |
| *s*(kJ/kg-K) | specific entropy |
| *h*(kJ/kg) | specific enthalpy |
| *T*(K) | temperature |
| $T_H$(K) | top cycle temperature |
| $T_L$(K) | bottoming cycle temperature |
| *u*(kJ/kg) | specific internal energy |
| *v*($m^3$/kg) | specific volume |
| *V*($m^3$) | volume |
| *w*(kJ/kg) | specific work |
| $w_i$(kJ/kg) | specific work input |
| $w_{iFP}$(kJ/kg) | Work added to drive the feed pump responsible to transfer the TWF |
| $w_o$(kJ/kg) | specific work out |
| $w_{oexp}$ (kJ/kg) | Output expansion work due to previously added heat |
| $w_{ocont}$ (kJ/kg) | Output contraction work due to previously extracted heat |
| $w_{oexp23}$ (kJ/kg) | Output expansion work $w_{o23}$ due to previously added heat |
| $w_{ocont41}$ (kJ/kg) | Output contraction work $w_{o41}$ due to previously extracted heat |
| $w_n$ (kJ/kg) | Net useful work ($w_{oexp}$ + $w_{ocont}$) = ( $w_{o23}$ + $w_{o41}$) |
| $q_{rec}$/PUi[kJ/kg] | Heat recovered from every PU from cooling cycles processes |
| $T_{q\_rec}$/PUi [K] | Temperature of the heat recovered from cooling cycles processes in every PU |
| *TF (%)* | Heat transfer losses due t heat recovery effectiveness |
| *LF* (%) | Losses factor (thermal and mechanical irreversibilities) |
| $\eta_{th}$ (%) | Cycle thermal efficiency [$w_n$/qi] |

**1 Introduction**

Starting from the general objective of establishing the design methodology for prototyping a self-sustained thermoelectric plant (characterized by not needing the assistance of any type of fuel or external energy source), two aspects inherent to the techniques of converting heat into work are essentially combined, which despite being known for more than a century, have not been taken into consideration for the design and development of efficient and technically disruptive power units (PUs), which are necessary to implement self-sustained power machines or thermoelectric plants (SSPM), which is the final objective of the proposed work.

Among the aspects considered, the following stand out:

-- work due to vacuum and atmospheric back-pressure used in both alternative steam engines that obey the developments of Savery [1], Newcomen [2] and Watt [3],, as well as conventional rotary steam engines (high-pressure steam turbines), which include the Rankine steam and organic Rankine thermal cycles. In all of them, a vacuum is used to increment the thermal efficiency.

-- work due to thermal contraction, characterized by a pressure lower than the reference pressure. The reference pressure is usually higher than the atmospheric pressure. When the reference pressure is equal to atmospheric pressure, the contraction pressure consists of a vacuum.

Regarding vacuum, it is convenient to highlight that, based on experimental observations when a thermal fluid contained in a closed space is cooled due to heat extraction, its temperature and pressure decrease, creating a vacuum, as well as its entropy. If the space is allowed to change its volume by means of a displacement of a piston and its rod, then it can produce useful mechanical work while the entropy decreases. That is, entropy can decrease while doing useful work.

The idea that vacuums or contraction pressure (any pressure lower than atmospheric pressure or lower than the initial or reference pressure of a contraction-based thermal cycle) can be used to perform useful mechanical work in heat engines is an ancient concept. Practical vacuum systems are available for carrying out useful mechanical work using vacuums obtained by cooling a TWF in several ways. For instance, some vacuum systems undergo a change of state via the condensation of the TWF (from steam to liquid water), which can be carried out in both open and closed processes.

Considering the fact that useful work by contraction is obtained when entropy is quasi-constant in the cases of adiabatic contraction, is evident by observation, and this transformation doesn't violate the second law of thermodynamics. Nevertheless, it is the key to achieving a thermal machine that uses a vacuum to carry out useful mechanical work via the thermal contraction of the TWF. If strictly adiabatic expansion and contraction are added to this technique, highly disruptive and efficient thermal machines are achieved.

Based on vacuum-based operating techniques, it has been possible to implement several reciprocating steam engines enabled to operate at atmospheric pressure. This advance was initially due to Savery, Newcomen and Watt [1-3]. Recently, Gerald Müller [4] presented an innovative concept concerning low-temperature-based atmospheric steam engines. The author extended the theory of the atmospheric steam engine operating under a vacuum (contraction) achieved by heat extraction to show that operation is possible at temperatures between 60 °C and 100 °C, although efficiency is further reduced as the temperature increases.

Similarly, Gerald Müller and George Parker [5] conducted a series of experiments to assess this theory by including a forced expansion stroke. Recently, the atmospheric steam engine (which implies that useful work is due to the presence of a vacuum) was re-evaluated. According to the authors, the theoretical efficiency of the ideal engine can be increased from 6.5% to 20%. Vítor Augusto Andreghetto Bortolin et.al. [6], developed a thermo dynamical model of an atmospheric steam engine, yielding acceptable results.

R. Ferreiro et al. [7-11] presented state-of-the-art technologies for thermal cycles that allow operation with closed processes of both thermal expansion and contraction.

Some interesting topics that has been taken into account deals with three disruptive technological challenges that must be overcome to implement efficient power units (PUs) capable of being operated by means of thermal contraction based on a vacuum under closed processes-based adiabatic-isentropic transformations, due to R. Ferreiro et al. [12-13] as well as optionally contraction based on strictly isothermal closed processes. The first challenge is that a thermal machine must be able to operate with the aforementioned thermal cycle (i.e., it must be capable of operating through thermal contraction). The second challenge is that the thermal cycles of a thermal machine must be able to operate with strictly isothermal processes of both thermal expansion and contraction. The third technological challenge is that a thermal machine must be able to develop highly effective forced thermal convection heat transfer media at the transfer rate required by the nominal power of each PU, where every PU is composed of a pair of RDACs equipped with associated heat transfer equipment.

Mentioned contributions were recently followed by advances on power plants composed bi groups of power unites coupled in cascade where, R. Ferreiro et al. [14-17], in which regenerative expansion-contraction-based cycles Power Plants have been researched. The data on the studied thermal real working fluids to be applied on the studied cases is achieved from E. W. Lemmon et. al [18].

The present study is focused on improving the efficiency of Power Plants in which instead of using heat regeneration in the PUs, cascade heat recovery is used, thereby achieving absolutely disruptive efficiencies compared to conventional technologies. The studied cases regarding to the prototyping tasks belong to patents referenced in [19-21].

Thus, based on the references [14-17], the design of two physical configurations of SSPMs enabled to widely exceed the nominal design powers is proposed, making use of the patents [19-21]. Therefore the two main prototype types proposed to demonstrate these capabilities include:

A continuous motion sVsVs thermal cycle prototype to operate the thermo-mechanical or thermo-hydraulic actuators with TWF reservoirs outside the thermal actuators.

A discontinuous motion VsVs thermal cycle prototype to operate the thermo-mechanical or thermo-hydraulic actuators inside the thermal actuators.

**2. Structure of PUs composed by reciprocating double-acting actuators (RDAA)**

The task of prototyping a self-sustaining power machine using cascaded Power Units (PUs) depends on the characteristics of each PU, which can be implemented under two main structural types of reciprocating double-acting actuators (RDAAs). These types relate to the volumetric reservoirs of thermal working fluid (TWF), which can be installed either outside the RDAAs, as shown in Fig.s 1(a), (b), and (c), or inside each reciprocating double-acting cylinder (RDAC), as illustrated in Fig. 2(a).

The design criterion for the RDAA regarding the location of the volumetric reservoirs of TWF is influenced by the type of displacement movement of the piston, which can be either continuous or discontinuous. To facilitate effective heat transfer to the TWF through forced thermal convection (FTC) while the actuator remains in continuous motion, it is necessary for the TWF reservoirs to be installed externally to the RDAC, as depicted in Fig.s 1(a), (b), and (c). Conversely, to achieve effective heat transfer through FTC when the actuator is at rest, the TWF reservoirs should be installed internally within the RDAC, as shown in Fig. 2(a).This indicates that the location of the TWF reservoirs determines the mode of movement of the reciprocating actuator (continuous or discontinuous). Therefore, to achieve continuous movement with reservoirs of TWF located inside the RDAC, as illustrated in Fig. 2(a), two RDACs must operate in a discontinuous and intermittent manner. This configuration ensures that when one RDAC is at rest, the other is in motion, and vice versa.

Therefore, scheduling the necessary prototyping tasks the following topics related to the above concepts must be addressed.

1 Main difference between the two structural types of RDAAs,

2 Influence of the location of the TWF reservoirs on the performance of the power machine,

3 Importance of FTC for effective heat transfer in these systems

4 Advantages of having the TWF reservoirs installed externally versus internally

5 Influence of the displacement movements of the piston on the design criteria of the RDAA.

**2.1 Structure of PUs composed by continuous-motion RDAA equipped with ETWFRs**

The PUs composed by continuous-motion RDAAs are necessarily equipped with ETWFRs being characterized by doing work by expansion and contraction under continuous motion. They obey the disruptive technology patented under the application numbers P201700667 reference [19] and P201700718 reference [20] illustrated in Fig. 1(a) (b) and (c). The design requirements to provide continuous motion demand that the heat addition and extraction tasks through forced thermal convection be carried out in thermal reservoirs located externally to the cylinder or actuating hydraulic system. This strategy ensures continuous movement of the piston while the thermal working fluid is heated and cooled at a constant volume. Satisfying such design conditions, it is possible to carry out a thermal cycle of the type sVsVs. Such types PUs installation requires a feed pump to return the expanded TWF again to the isochoric heating system.

As depicted in Fig. 2(a), a single discontinuous motion RDAC with ITWFRs is equipped with heat transfer accessories including heat addition and heat extraction equipment. In addition, the discontinuous RDAC is coupled to a reciprocating double-acting hydraulic pump enabled to drive a rotary hydraulic motor-generator coupled to a generator. In Fig. 2 (b) it is depicted the scheme of a discontinuous-motion RDAHyR equipped with the necessary hydraulic flow control valves enabled to drive a rotary hydraulic motor-generator coupled to a generator.

The continuous-motion PUs composed of two discontinuous-motions actuator is depicted in Fig. 3. Therefore, Fig. 3(a) shows the discontinuous-motion RDAC coupled to a RDAHyP to drive a rotary hydraulic motor-generator coupled to a generator, and Fig. 3(b) shows the discontinuous RDAHyRs to drive a rotary hydraulic motor-generator mechanically coupled.

Each PU, characterized by having volumetric reservoirs of the TWF inside the RDAA, exhibits the characteristic of disabling the TWF feed pump. In turn, this characteristic necessarily requires intervals of dynamic inactivity of the actuator to allow heat transfer to the TWF. Then, the time elapsed during the simultaneous processes of isochoric addition and extraction of heat to/from the TWF inside the RDAA, requires that it remain stationary (without performing either expansion or contraction work) to favor heat transfer in both the heat addition and extraction processes. To compensate and eliminate the RDAA inactivity time interval, and achieve continuous movement, it is proposed to duplicate each RDAA in such a way that when one of them acts performing expansion or contraction work, its complementary RDAA remains stationary transferring heat and vice versa.

The completion of any RDAA is achieved by implementing two types of thermo-mechanic-hydraulic actuation according to patent P02200035 reference [21].

-- The option illustrated in Fig. 1(b), consist of a PU based on patents [19-21], equipped with RDAC coupled to a double-acting reciprocation hydraulic pump according to patent [21].

-- The option illustrated in Fig. 1(c), consisting of a PU based on patents [21]. equipped with ETWFRs directly coupled to a reciprocating double thermo-hydraulic actuator based on RDAHyR according to patent [21].

The continuous-motion RDAA equipped with ETWFRs depicted in Fig. 1 is composed at least with the following components: Fig. 1(a) shows a PU based on references [19-20] equipped with ETWFRs, equipped with RDAC

based on thermo-mechanic actuation. (b), shows a PU based on patents [19-21] which uses ETWFRs, and is equipped with RDAC based on thermo-mechanic-hydraulic actuation according patent [21], and (c) shows a PU based on patents [19-21]. It is, equipped with ETWFRs coupled to a reciprocating thermo-hydraulic actuator based on RDAHyR according to patent [21]. Finally Fig. 1(d) shows the symbol to represent each PU operating with a cycle sVsVs of the type shown in Fig.s 1(b) and 1(c).

The completion of any RDAA is achieved by implementing two types of thermo-mechanic-hydraulic actuation according to patent [21]. Therefore, the option illustrated in Fig. 1(b), consisting of a PU based on patents [19-21] which is equipped with RDACs coupled to a double-acting reciprocation hydraulic pump according to patent [21]. The option illustrated in Fig. 1(c), consist of a PU based on patent [21] which is equipped with ETWFRs directly coupled to a reciprocating double thermo-hydraulic actuator based on RDAHyR according to patent [21].

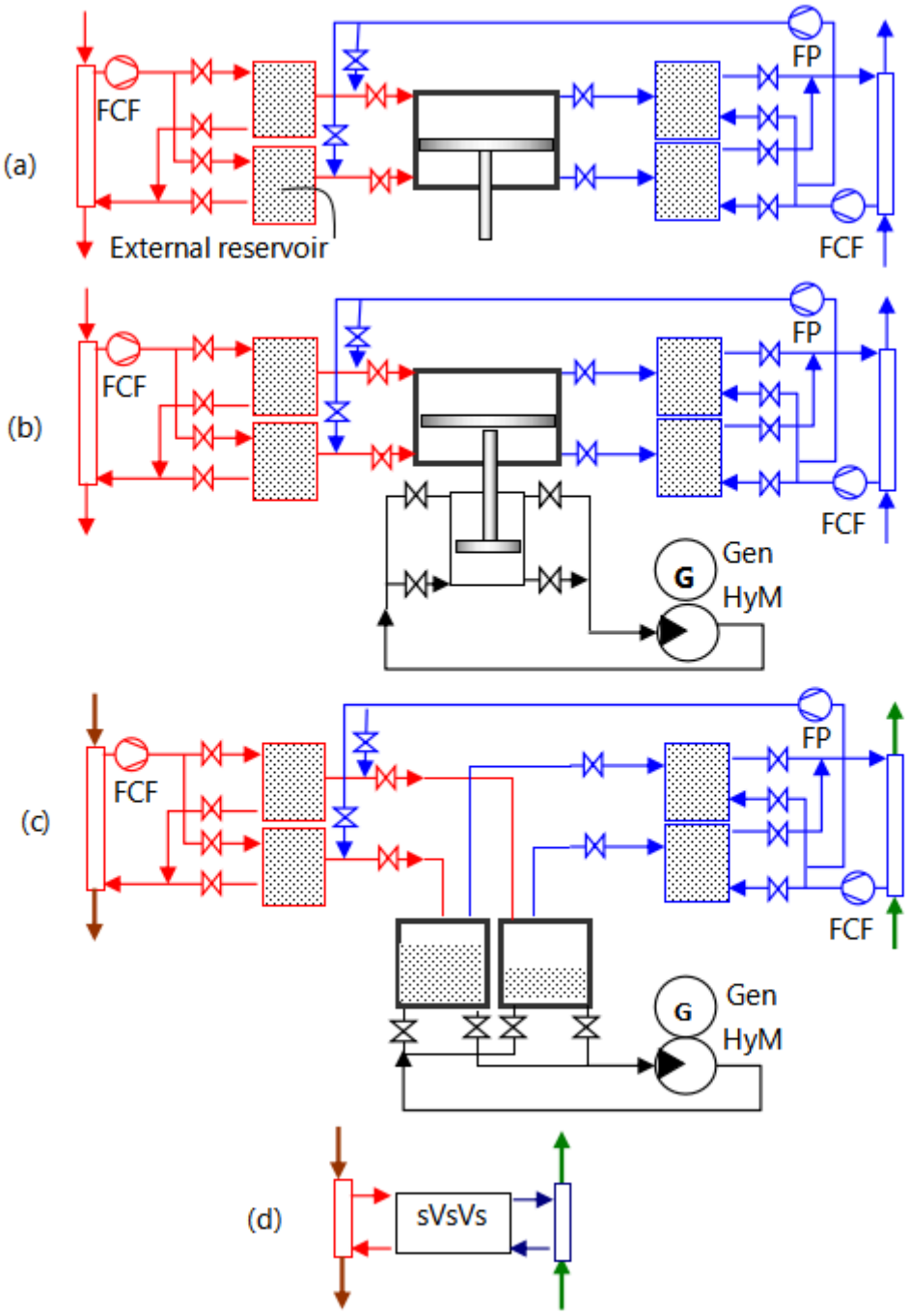


Fig. 1: Illustration of the schematic structure of a continuous-motion RDAA equipped with ETWFRs.

**2.2 Structure of PUs composed by discontinuous-motion RDACs equipped with ITFR**

The task of prototyping a self-sustaining power machine by means of cascaded power units composed of RDAA based on discontinuous motion-based actuators are characterized by doing work by expansion and contraction. These types relate to the volumetric reservoirs of TWF, which is necessarily installed inside each RDAA: That means inside each RDAC or inside each RDAHyR as illustrated in Fig. 2(a) and (b) respectively. Mentioned prototyping options obey the disruptive technology patented under the application number P202200035.

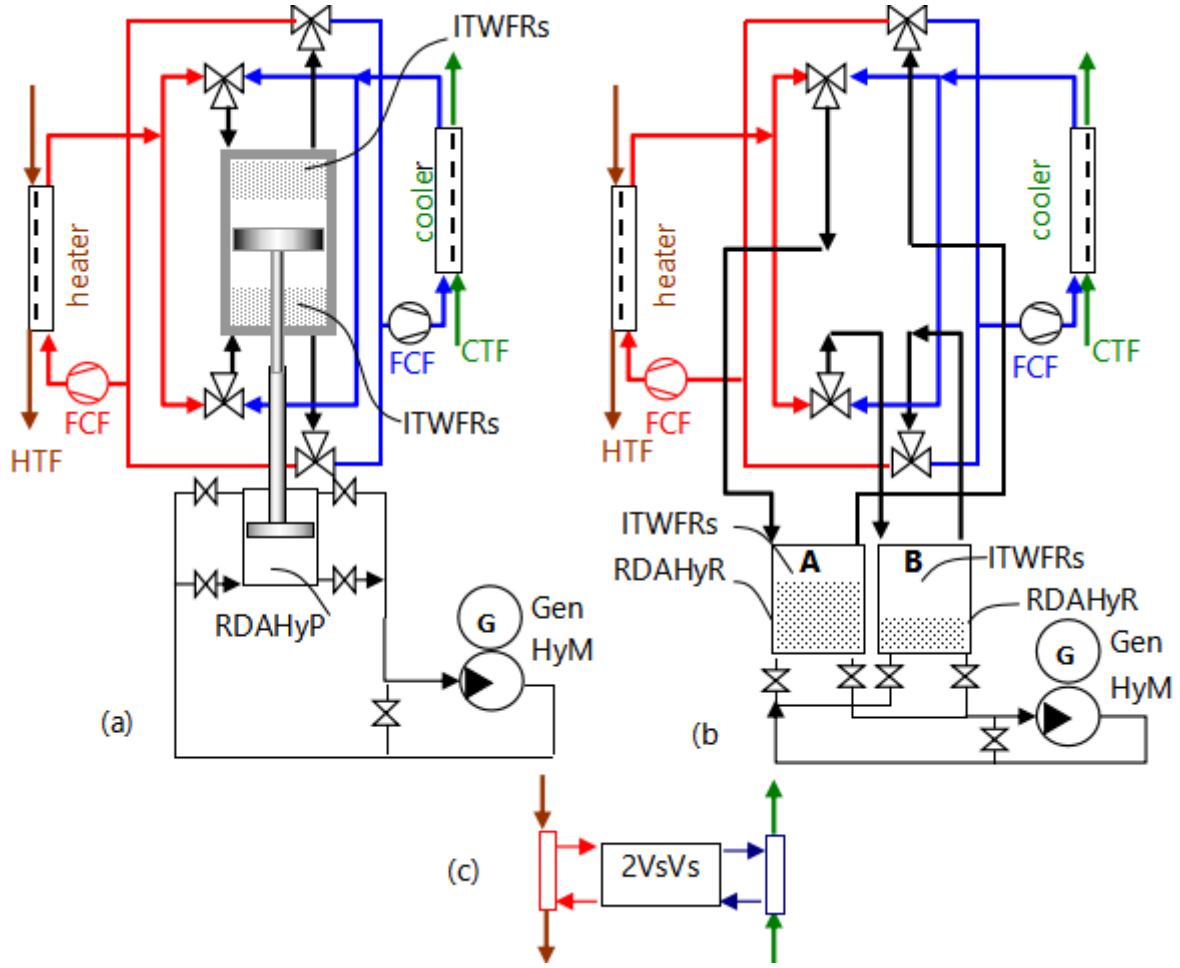


Figure 2: Schematic structure of a discontinuous-motion RDAA equipped with ITWFRs. (a), Discontinuous RDAC coupled to a RDAHP enabled to drive a rotary hydraulic motor-generator. Patent P202200035. (b), Discontinuous RDAHyRs to drive a rotary hydraulic motor-generator. (c), symbol to represent each PU operating with a cycle VsVs of the type shown in 2(a) and 2(b).

The installation proposed to overcome the inconvenience caused by time intervals elapsed during heat transfer giving rise to inactivity intervals is shown in Fig. 3(a) and (b).

This means that each PU requires two RDAAs connected in parallel with respect to the heat addition and extraction circuits.

In summary, prototyping a continuous motion PU with a feed pump requires the installation of external reservoirs; while exhibiting continuous motion capability with reservoirs inside each RDAA requires two RDAA units to complete each continuous motion PU.

**3 Thermal cycles applied on the proposed continuous and discontinuous motion-based prototypes**

The prototypes proposed in sections 2.1 and 2.2 must operate with thermal cycles adapted to each of the two prototyped models, depending on design factors such as:

--location of reservoirs (internal or external to the actuators),

--RDAA such as (thermo-mechanical or thermo-hydraulic actuators),

--Motion types such as (intermittent continuous motion, among other factors).

.

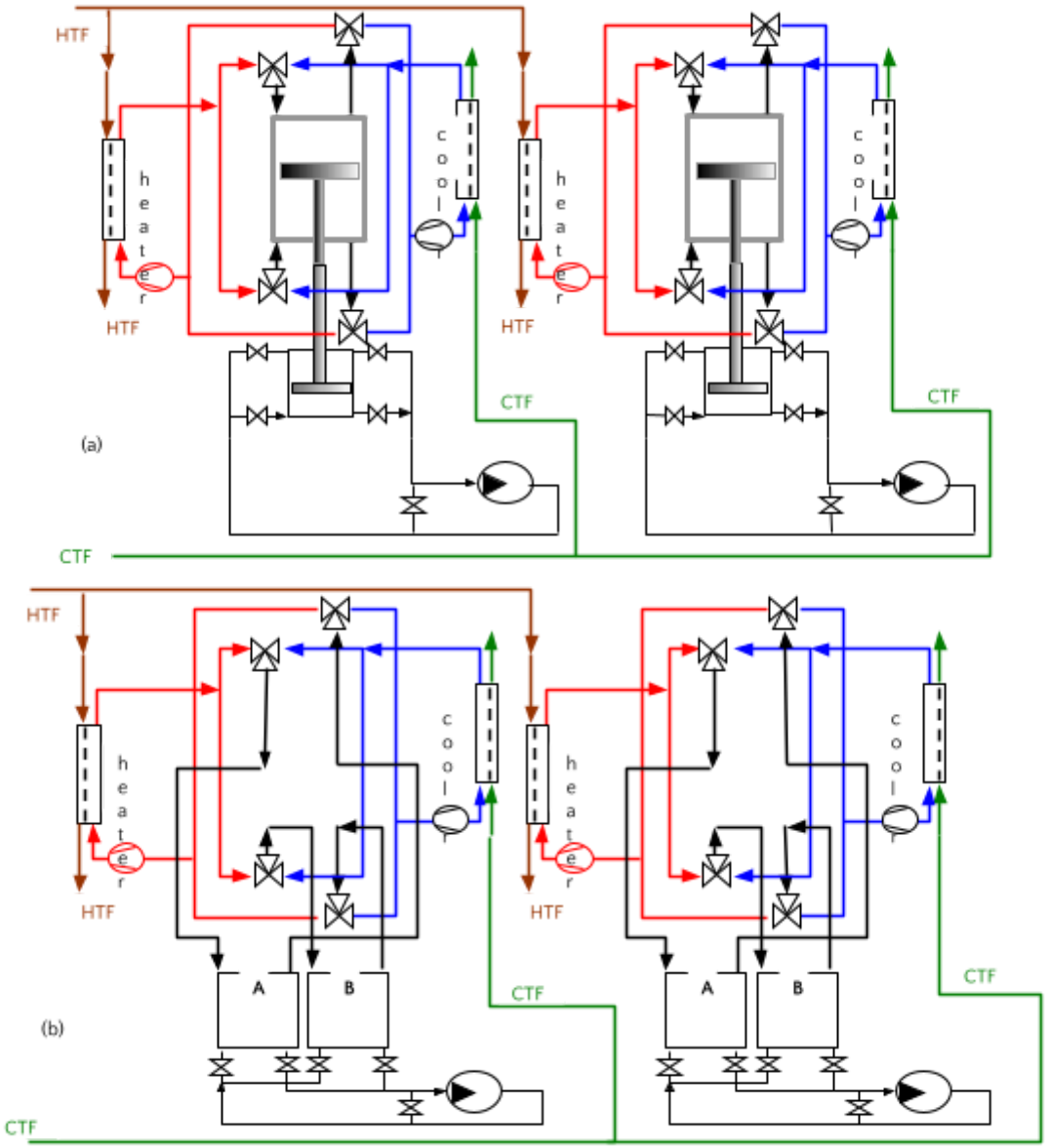


Figure 3: Continuous-motion PUs composed of two discontinuous-motions actuators, each equipped with heat supply and heat recovery piping systems, according to patent P202200035.

In this sense, thermal cycles enabled to operate with adiabatic-isentropic and isochoric thermal processes are selected. Such considered cycles are characterized by completing a thermal cycle by means of adiabatic-isentropic and isochoric transformations. This option allows heat to be added with minimum energetic effort, while it is converted to useful work by expansion and contraction free of additional interactions.

The name of the cycle sVsVs obeys the thermodynamic transformation involved in each thermal cycle. The following nomenclature depicted in the above list is used along the studied thermal cycles considered in the paper:

| **Cycle transformations** | **Process type** | **Acronym** |
|---|---|---|
| isentropic-adiabatic | constant entropy (no heat transfer) | s |
| isochoric | constant volume | V |
| Isothermal | constant temperature | T |
| isobaric | constant pressure | p |

Thus, the cycle depicted in above list operates with only two thermodynamic transformations: adiabatic-isentropic (s) and isochoric (V). Since these processes must be performed to obtaining expansion and contraction works, a complete cycle requires the following constant variable processes: **s**, **V**, **s**, **V** and **s**, so that it is named as **sVsVs** cycle.

**3.1 Cycle transformations for the sVsVs continuous motion prototype**

Regarding the information provided in Table 1, Fig. 1 (a), (b) and (c), and Fig. 4 (a) and (b), the thermodynamic transformations carried out between each pair of state points of the cycle performed in the cylinder chamber A of the RDAC are summarized as follows:

*Process (1)-(2)* corresponds to an open adiabatic compression process to drive the thermal working fluid feed pump. The amount of work added to a feed pump under an adiabatic-isentropic process is

$$w_{i12} = h_2 - h_1 = Cp \cdot (T_2 - T_1) \tag{1}$$

*Process (2)-(3)* corresponds to a closed isochoric heat addition process in which the TWF is heated according to the heat transfer model:

$$q_{i23} = \Delta u_{23} = u_3 - u_2 = Cv \cdot (T_3 - T_2) \tag{2}$$

*Process (3)-(4)* corresponds to a closed adiabatic expansion process (cylinder chamber volume increases due to the piston displacement). Thus, the thermal energy in the form of internal energy is converted into mechanical work, provided that the piston can move freely doing the expansion work.

$$w_{o34} = w_{o\exp} = u_3 - u_4 = Cv \cdot (T_3 - T_4) \tag{3}$$

*Process (4)-(5)* corresponds to a closed isochoric heat extraction process in which the working fluid is cooled without work done because of the constant volume process:

$$q_{o45} = \Delta u_{45} = u_3 - u_4 = Cv \cdot (T_4 - T_5) \tag{4}$$

*Process (5)-(1)* corresponds to a closed adiabatic contraction-based compression process. Thus, the thermal energy in the form of internal energy is converted into mechanical work by contraction (cylinder chamber volume decreases due to piston displacement), provided that the piston can move freely to permit the contraction work.

$$|w_{o51}| = |w_{ocont}| = |u_5 - u_1| = Cv \cdot |(T_5 - T_1)| = Cv \cdot |(T_1 - T_5)| \tag{5}$$

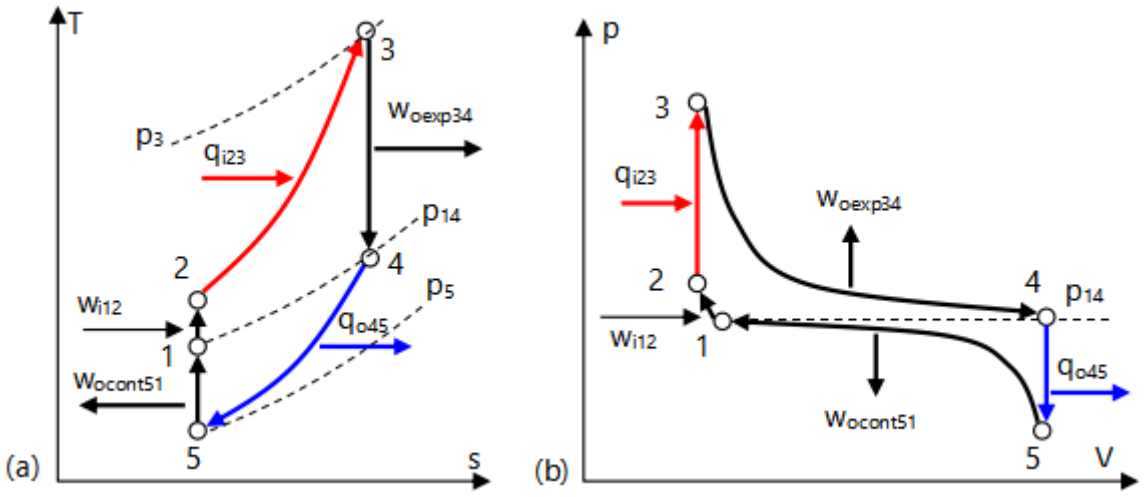


Figure 4: Single sVsVs (closed processes-based thermal cycle. (a): T-s diagram. (b): p-V diagram

Table 1: Cycle transformations carried out in the sVsVs cycle showing the thermodynamic functions carried out simultaneously in both RDACs chambers (A) and (B). The table also depicts the useful work, constant parameters and heat transfer direction associated with each transformation according to Equations (1-9).

| **sVsVs** cycle: cylinder chamber **A** | | | | **sVsVs** cycle: cylinder chamber **B** | | | |
|---|---|---|---|---|---|---|---|
| sp | useful work | constant | heat in/out | sp | useful work | constant | heat in/out |
| 1-2 | $-w_{i2}=\Delta h_{12}$ | s | | 2'-3' | | V | $q_{i23}=\Delta u_{23}$ |
| 2-3 | | V | $q_{i23}=\Delta u_{23}$ | 3'-4' | $w_{o34}=\Delta u_{34}$ | s | |
| 3-4 | $w_{o34}=\Delta u_{34}$ | s | | 4'-5' | | V | $q_{o45}=\Delta u_{45}$ |
| 4-5 | | V | $q_{o45}=\Delta u_{45}$ | 5'-1' | $w_{o51}=\Delta u_{51}$ | s | |
| 5-1 | $w_{o51}=\Delta u_{51}$ | s | | 1'-2' | $-w_{i2}=\Delta h_{12}$ | s | |

Table 1 shows the cycle transformations presented in Equations (1) – (5) carried out in each actuator-based cylinder chamber. The table also depicts the useful work, constant parameters, and heat transfer direction associated with each transformation.

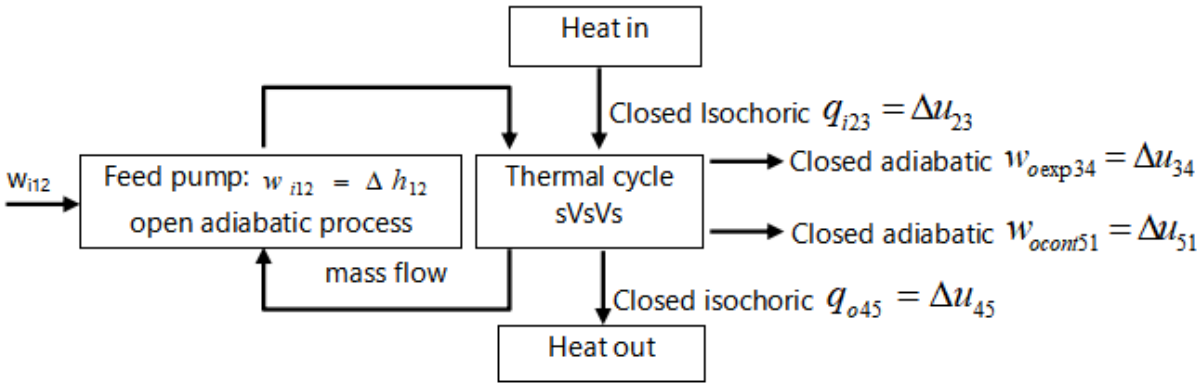


Figure 5: sVsVs thermal cycle energy (heat-work) flow diagram doing work by open adiabatic expansion and contraction while transferring heat by closed isochoric heat addition and heat extraction during.

Fig. 5 depicts the energy flow-chart associated with the transformations carried out along the thermal cycle sVsVs. It is observed that the work added to the feed pump is processed under thermodynamic open system, while the rest of the cycle processes (useful work obtained, heat added and heat extracted) are carried out under thermodynamic closed systems.

**3.1.1 Cycle sVsVs analysis of a continuous motion prototype**

The analysis of the proposed cycle is based on the first law such that the energy transfer flows include the following energy balances derived from the previous section:

*Added input heat*

$$q_i = u_3 - u_2 = Cv \cdot (T_3 - T_2) \tag{6}$$

*Extracted output heat*

$$q_o = u_4 - u_5 = Cv \cdot (T_4 - T_5) \tag{7}$$

*FP work assumed as added input work*

The input work is due to the working fluid transfer by a feed compressor. The analysis is simplified without a loss of generality by considering the amount of work due to the compression of the working fluid as follows:

$$w_{i12} = h_2 - h_1 = \Delta h_{21} = Cp \cdot (T_2 - T_1) = Cp \cdot \Delta T_{21} \tag{8}$$

The required work used to drive the forced convection circulation fans (one per heat exchanger not represented in Figs. 4 and 5) is neglected in this analysis.

*Output work*

$$\begin{aligned} w_o &= w_{o\exp} + |\, w_{ocont} \,| = w_{034} + w_{o51} = \\ &Cv \cdot (T_3 - T_4) + Cv \cdot |\, (T_5 - T_1) \,| = \\ &= (u_3 - u_4) + |\, (u_5 - u_1) \,| \end{aligned} \tag{9}$$

*Net useful work*

$$w_n = w_{o\exp} + |\, w_{ocont} \,| - w_{i12} = (u_3 - u_4) + |\, (u_5 - u_1) \,| - \Delta h_{12} \tag{10}$$

Therefore, the thermal efficiency is given by the ratio of the net mechanical work to the added input heat, yielding

$$\eta_{th} = \frac{w_n}{q_i} = \frac{w_{o34} + |\, w_{o51} \,| - \Delta h_{12}}{u_3 - u_2} = \frac{(u_3 - u_4) + |\, (u_5 - u_1) \,| - \Delta h_{12}}{u_3 - u_2} = \tag{11}$$

**3.2 Cycle transformations for a VsVs discontinuous motion prototype**

Regarding the information provided in Table 2 and Fig.. 2 (a), (b), and Fig. 6 the thermodynamic transformations between each pair of state points of the cycle carried out on the left side of the discontinuous RDAC are summarized as follows:

*Process (1)-(2)* corresponds to a closed isochoric heat addition process in which the TWF is heated according to the heat transfer model:

$$q_{i12} = \Delta u_{12} = u_2 - u_1 = Cv \cdot (T_2 - T_1) \tag{12}$$

*Process (2)-(3)* corresponds to a closed adiabatic expansion process (cylinder chamber volume increases doing work). Thus, the thermal energy in the form of internal energy is converted into mechanical work, provided that the piston can move freely to permit the expansion work.

$$w_{o23} = w_{o\exp} = u_2 - u_3 = Cv \cdot (T_2 - T_3) \tag{13}$$

*Process (3)-(4)* corresponds to a closed isochoric heat extraction process in which the working fluid is cooled without any work being done because of the constant volume process:

$$q_{o34} = \Delta u_{34} = u_3 - u_4 = Cv \cdot (T_3 - T_4) \tag{14}$$

6++++

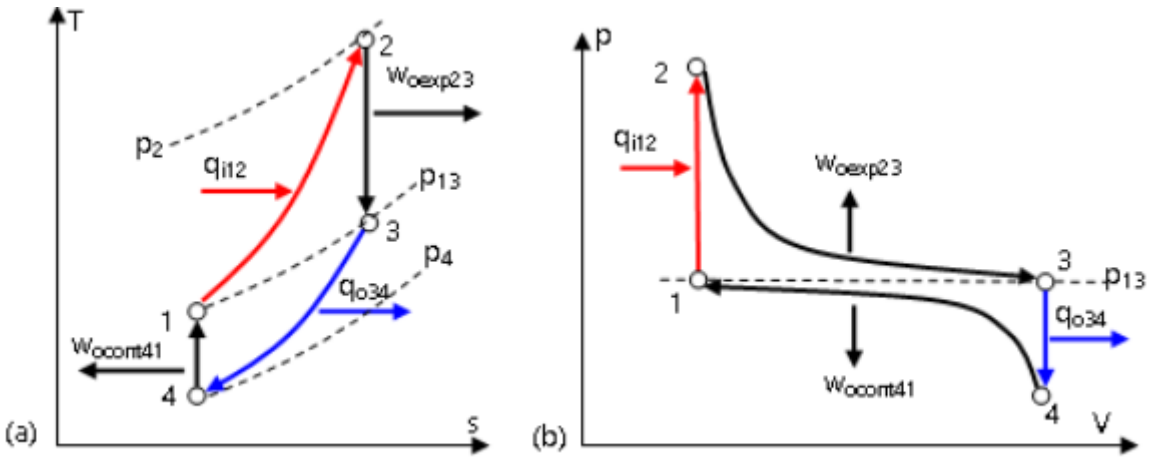


Figure 6: Single VsVs closed processes-based thermal cycle. (a): T-s diagram. (b): p-V diagram

*Process (4)-(1)* corresponds to a closed adiabatic contraction-based compression process. Thus, the thermal energy in the form of internal energy is converted into mechanical work by contraction (cylinder chamber volume decreases doing work), provided that the piston can move freely to permit the contraction work:

$$| w_{o41} | = | w_{ocont} | = | u_4 - u_1 | = Cv \cdot | (T_4 - T_1) | = Cv \cdot | (T_1 - T_4) | \quad (15)$$

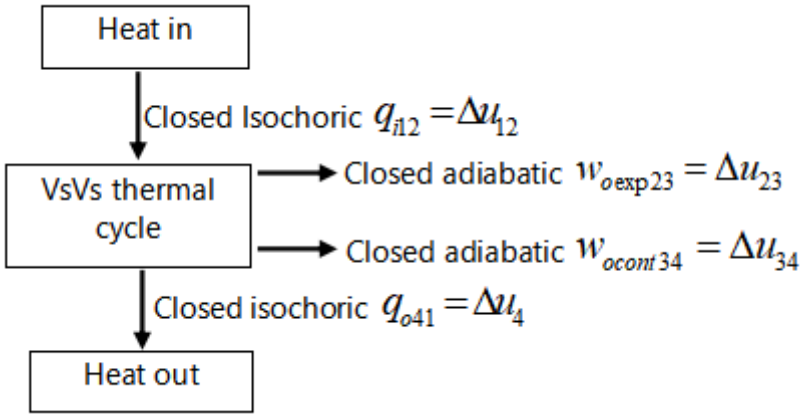


Figure 7: VsVs thermal cycle energy (heat-work) flow diagram doing work by closed adiabatic expansion and contraction while transferring heat by closed isochoric heat addition and heat extraction.

Fig. 7 depicts the energy flow-chart associated with the transformations carried out along the thermal cycle VsVs. It is observed that no feed pump is required, so that the cycle processes (useful work obtained, heat added and heat extracted) are carried out under thermodynamic closed systems.

Table 2: Cycle transformations carried out in the VsVs cycle showing the thermodynamic functions carried out simultaneously in both RDACs chambers (A) and (B). The table also depicts the useful work, constant parameters and heat transfer direction associated with each transformation according to Equations (12-17).

| **VsVs** Cycle performed: cylinder chamber **A** | | | | **VsVs** Cycle performed: cylinder chamber **B** | | | |
|---|---|---|---|---|---|---|---|
| sp | useful work | constant | heat in/out | sp | useful work | constant | heat in/out |
| 1-2 | motionless | V | $q_{i12} = \Delta u_{12}$ | 3'-4' | motionless | V | $q_{o34} = \Delta u_{34}$ |
| 2-3 | $w_{o23} = \Delta u_{23}$ | s | $q_{i23} = \Delta u_{23}$ | 4'-1' | $w_{o41} = \Delta u_{41}$ | s | $q_{o41} = \Delta u_{41}$ |

| | | | | | | | |
|---|---|---|---|---|---|---|---|
| 3-4 | motionless | V | $q_{o34} = \Delta u_{34}$ | 1'-2' | motionless | V | $q_{i12} = \Delta u_{12}$ |
| 4-1 | $w_{o41} = \Delta u_{41}$ | s | $q_{o41} = \Delta u_{41}$ | 2'-3' | $w_{o23} = \Delta u_{23}$ | s | $q_{i23} = \Delta u_{23}$ |

**3.2.1 Cycle analysis of a VsVs discontinuous motion prototype**

The cycle analysis is based on the first law. Thus, the energy transfer flows include the following energy balances derived from the previous section:

*Added input heat*

$$q_i = q_{i12} = u_2 - u_1 = Cv \cdot (T_2 - T_1) \tag{16}$$

*Extracted output heat*

$$q_o = q_{o34} = u_3 - u_4 = Cv \cdot (T_3 - T_4) \tag{17}$$

*Net useful output work*

$$w_o = w_{o\exp} + |\, w_{ocont} \,| = Cv \cdot (T_2 - T_3) + Cv \cdot |\, (T_4 - T_1) \,|$$
$$= (u_2 - u_3) + |\, (u_4 - u_1) \,| \tag{18}$$

Therefore, the thermal efficiency is given by the ratio of the net mechanical work to the added input heat, yielding

$$\eta_{th} = \frac{w_n}{q_i} = \frac{w_{o23} + |\, w_{o41} \,|}{u_2 - u_1} = \frac{(u_2 - u_3) + |\, (u_4 - u_1) \,|}{u_2 - u_1} \tag{19}$$

However, since an important fraction of the useful work is carried out by a vacuum or thermal contraction, it is interesting to consider the proportions of useful work obtained by thermal contraction due to cooling concerning those obtained by thermal expansion.

**3.3 Influence of cycle temperature ratios of each PU on the SSPM performance**

Every PU proposed to implement a SSPM completes a sVsVs cycle or a VsVs cycle by executing two simultaneous sVsVs-type or VsVs-type cycles. Both thermal cycles are executed in such a way that when one of the thermal cycles sVsVs is doing useful mechanical work due to expansion and contraction simultaneously, the complementary thermal cycle is in the phase of heat addition and extraction simultaneously.

To continue the study of the SSPM, it is necessary to know the characteristics of each PU, which depend on the thermodynamic characteristics of the considered thermal cycle. Thus, in order to know the behavior of the sVsVs and VsVs thermal cycles with respect to the Ratio of Isochoric Temperatures (RIT) the following characteristic distinction must be considered

Case of **sVsVs** cycle: RIT = $T_1/T_3$

Case of **VsVs** cycle: RIT = $T_1/T_2$

The optional value of RIT is chosen fulfilling a criterion such that they provide an acceptable performance of each cascaded PU. Thus, the search is based on the definition of the relationship of temperatures in a similar application range to that expected for operating in the desired SSPM when PUs are coupled in cascade downstream.

**3.3.1 Definition of the RIT for continuous-motion cycle sVsVs**

From equations (3) and (5) we have

$$w_{o\exp 34} = Cv \cdot (T_3 - T_4) \tag{20}$$

$$w_{ocont51} = Cv \cdot (T_1 - T_5) \tag{21}$$

From (20) and (21) it is achieved the isochoric temperatures as

$$T_3 = \frac{w_{o\exp 34} + Cv \cdot T_4}{Cv} \tag{22}$$

$$T_1 = \frac{w_{ocont51} + Cv \cdot T5_5}{Cv} \tag{23}$$

Thus, the ratio of the isochoric temperatures *RIT* is

$$RIT = \frac{T_1}{T_3} = \frac{w_{ocont51} + Cv \cdot T_5}{w_{o\exp 34} + Cv \cdot T_4} \tag{24}$$

To observe the relevance of selecting an appropriate RIT value under efficiency criteria apart from other operating parameters such as cycle reference pressure and maximum pressures, the following case study on the PGT-sVsVs cycle is carried out.

**3.3.2 Definition of the RIT for discontinuous-motion cycle VsVs**

From equations (13) and (15) we have

$$w_{o\exp 23} = Cv \cdot (T_2 - T_3) \tag{25}$$

$$w_{ocont41} = Cv \cdot (T_1 - T_4) \tag{26}$$

From (25) and (26) it is achieved the isochoric temperatures as

$$T_2 = \frac{w_{o\exp 23} + Cv \cdot T_3}{Cv} \tag{27}$$

$$T_1 = \frac{w_{ocont41} + Cv \cdot T5_4}{Cv} \tag{28}$$

Thus, the ratio of the isochoric temperatures *RIT* is

$$RIT = \frac{T_1}{T_2} = \frac{w_{ocont41} + Cv \cdot T_4}{w_{o\exp 23} + Cv \cdot T_3} \tag{29}$$

**3.3.3 Analysis of the RIT**

The analysis of the RIT behavior as a function of the extreme temperatures of the isochoric processes of the sVsVs and VsVs cycles is very useful to determine the operating temperatures such that the work obtained by contraction reasonably approximates the work obtained by expansion of the TWF. The objective is to achieve a high thermal efficiency of the thermal cycle associated with each PU while the SSPM is implemented with the minimum number of PUs coupled in cascade.

Thus, from Equations (24) and (29), it is deduced that under this condition, the work achieved by contraction approaches the work achieved by expansion, which approaches the maximum achievable thermal efficiency. However, real systems are subject to all types of irreversibilities due to the inherent interaction of non-conservative forces. Since the maximum value of the RIT occurs for $T_1 = T_3$ in the case of sVsVs cycle or for $T_1 = T_2$ in the case of VsVs cycles, the desired value of the RIT is the one that allows obtaining the greatest efficiency in a range of real PUs, typically found in the range of values between 0.80 and 0.95. A high RIT value will require a larger number of cascaded PUs, while a lower RIT value will require less PUs to complete a SSPM. Reference [9596].

Therefore, given the paramount importance of the RIT value selection in terms of the PUs performance as well as the influence on the complete SSPM performance, further study on its utilization is required. Thus, in order to investigate the behavior of the RIT let's to consider the definition achieved by Equation (29), since the results will be similar to those achieved from the Equation (24) due to the fact that the thermal cycles sVsVs and VsVs, in terms of heat transfer and work done are similar.

To determine the trend of the RIT function, it is necessary to take limits from Equation (29) proceeding as follows:

$$\lim_{T_2 \to T_1}[RIT] = \lim_{T_2 \to T_1}[\frac{T_1}{T_2}] = \lim_{T_2 \to T_1}[\frac{w_{ocont41} + Cv \cdot T_4}{w_{o\exp 23} + Cv \cdot T_3}] = 1 \quad (30)$$

Equation (30) means that when $T_2$=$T_1$ then

$$w_{ocont41} + Cv \cdot T_4 = w_{o\exp 23} + Cv \cdot T_3 \quad (31)$$

The consequence derived from Equation (31) is that under these conditions given as:

If $T_1 = T_2$ then $T_3 = T_4$, (32)

And consequently, from 31) follows that:

$$w_{ocont41} = w_{o\exp 23} \quad (33)$$

In summary, when RIT = 1, the expansion and contraction work are equal. Therefore, Equation (33) implies that under the conditions considered, the thermal efficiency of the PU in question is the maximum possible with respect to the added heat.

According to Equation (29), if $T_{23}$ tends to the value of $T_{41}$, then the work $w_{23}$ tends to the value of $w_{41}$. This means that when the ratio between $T_1$ and $T_2$ tends to one, the ratio between $W_{23}$ and $W_{41}$ also tends to one. In other words, a high value of the $T_1/T_2$ ratio results in a high ratio between the works $w_{23}$ and $w_{41}$.

Consequently, the next step involves the description of the prototype, in which the concept of RIT will be applied as a criterion for improving cycle efficiency in the considered case studies. Some key factors essential to achieve SSPMs with high SSI include:

1. A unified heat carrier circuit for the cascaded PUs, responsible for both adding and recovering heat efficiently and increasing their recovered heat potential by increasing their temperature.

2. The highest possible RIT to improve the efficiency of each individual PU and, consequently, the highest possible SSI value.

3. The task of supplying heat to the top PU in the cascade coupling structure is carried out using one of the available heat transfer techniques based on thermal energy superposition.

In the next section, the efficiency behavior of the PUs will be analyzed based on the optional RIT values.

**4 Validation of the sVsVs and VsVs cycles based on case studies**

The devices used to carry out the validation studies of the SSPMs equipped with cascaded PUs implemented with any RDAA differ from each other in that those operating in continuous motion mode require thermo-volumetric reservoirs external to the actuator, i.e. located outside the active volume (volume subject to expansion and contraction) of the actuator and require a TWF feed pump, while those operating in discontinuous motion mode require thermo-volumetric reservoirs inside the actuator and therefore located within the active volume of the actuator, thus not requiring a feed pump, which requires the thermal cycle to be carried out in a discontinuous manner to allow heat transfer to/from the actuator. This difference in structures gives rise to the need for two types of thermal cycles: sVsVs cycle and VsVs cycle.

The cases depicted in Tables 3 consists of the study of two SSPMs, each equipped with 5 continuous-motion thermal cycles of the type sVsVs operating respectively with helium and air as TWFs, while the cases depicted in Tables 5 consists of the study of two SSPMs, each equipped with 5 discontinuous-motion thermal cycles of the type VsVs operating respectively with helium and air as TWFs. In both cycle types the top temperature $T_3$ is fixed at 800 K for the sVsVs cycle and $T_2$ for the VsVs cycle. The temperature $T_1$ for each PU is fixed in a value such that, assuming the RIT as $T_1/T_3$,for the sVsVs cycle then, $T_1$ = RIT(PUi).$T_3$ or RIT as $T_1/T_2$ for VsVs cycle then $T_1$ = RIT(PUi).$T_2$. Thus, the selected RIT for each case considered is assumed as 0.85. Along the analysis carried out in this work, the thermodynamic data properties of the TWFs is taken from Lemmon E. W., et all, [19].

**4.1 Criteria to be taken into account when carrying out SSPM prototyping tasks**

The criteria to be taken into account obey to the previous studies along this work as well as previous results from references [14-18]. Therefore, the key innovative concepts proposed for improving thermal contraction efficiency in the SSPMs systems are summarized by four disruptive and strategic considerations:

a- Utilizing thermal contraction to generate useful work:

- The SSPM design leverages the thermal contraction of the working fluid, in addition to expansion, to generate efficiently useful mechanical work.
- Performing work through contraction is a critical mechanism that enables the SSPM to achieve remarkably high efficiencies and self-sufficiency on the basis of a proper selection of the RIT. This achievement is mainly due to the proper choice of RIT by which almost as much work can be obtained by thermal contraction based on cost-free heat extraction as by expansion due to heat addition, which entails costs inherent to the addition of heat.
- This contrasts with traditional power cycles that rely solely on expansion to produce work, apart from the fact that there is no possibility of using the concept of RIT, so that the plant structure based on cascaded PUs doesn't work at all. The main reason is that the heat rejected by the expansion becomes a low-grade heat, so that its recovery is inefficient.

b- Closed processes-based thermal cycles with expansion and contraction, without state changes (no condensing or vaporizing processes):

- The SSPM employs specialized thermal cycles, such as the sVsVs and VsVS cycles that operate through closed processes of both heat addition and heat extraction to perform closed processes-based thermal expansion and contraction. Closed processes are characterized by the lack of typical losses due to flow and isentropic work, which results in an increase in the efficiency of the heat-useful work conversion processes.
- This allows the system to extract useful work from both the expansion and contraction of the working fluid. This feature leads to the need for a selection of the optimal RIT value to efficiently exploit the assistance due to the performance of work by thermal contraction.

c- Disruptive strategy on efficient heat recovery and reuse tasks:

- The SSPM consisting of a group of cascaded PUs coupled in cascade recovers the heat resulting from the cooling process that drives the thermal contraction. The value of this heat represents almost half of the heat manipulated in heat-work conversion processes. This is why it is so important since it is obtained at no cost.
- This recovered heat will be then reintegrated to power the first PU in the cascaded system, enabling the "heat superposition" strategy on the basis of electric power to heat conversion which undergoes near 100% efficiency.
- This heat management approach allows the SSPM to generate more useful work than the initial heat input, exceeding 100% thermal efficiency.

d- Working Fluid Selection:

- The choice of working fluid, such as helium versus air, has a major impact on the thermal contraction efficiency and overall performance of the SSPM.
- Helium's superior thermodynamic properties allow it to extract significantly more useful work from the contraction process compared to air. This disruptive result implies the urgent need to revise some conventional axioms related to the fundamental principles of physics concerning thermodynamics.

Based on the criteria taken into consideration, in this same section the necessary studies are carried out for the design and implementation of the prototypes corresponding to two SSPM structures characterized by PUs consisting of thermo-hydraulic actuators equipped with volumetric heat reservoirs located inside and outside the thermo-actuator systems. Furthermore, having the reservoirs inside or outside the thermo-actuator systems implies the implementation of continuous and discontinuous thermal cycles.

**4.2 The structure of a SSPM based on Thermo-Hydraulic actuators**

The studies for the development of two main types of prototypes at simulation level are proposed. In such studies the necessary condition to satisfy the above-mentioned abilities have been imposed:

1 continuous motion with a thermal cycle of the sVsVs type and reservoirs of the thermal working fluid reservoirs located outside the thermomechanical or thermo-hydraulic actuators, illustrated in Fig.s 8(a) and (b).

2 discontinuous motions with a thermal cycle of the VsVs type and reservoirs of the thermal working fluid reservoirs located inside the thermomechanical or thermo-hydraulic actuators, illustrated in Fig.s 8(c) (d) and (e).

The SSPMs previously described in references [12-13] consist of double-acting reciprocating machines characterized by some implementation technical difficulties regarding the coupling of movements and the uniform distribution of output forces towards a common eclectic generator.

In these prototypes, it is intended to eliminate such drawbacks by simplifying the installation by means of a common mechanical coupling consisting of a shaft comprising all the plant-based PUs driving an unique electric generator.

**4.2.1 Design task considerations**

An SSPM (Self-Sustaining Power Machine) must be characterized by its ability to operate indefinitely without an external energy input [11-13]. This essential characteristic must overcome the irreversibilities inherent in any real machine. This means it must surpass the limitations of second-kind perpetual motion machines, whose operation involves a combination of mechanical and thermal transformations that are inherently affected by dissipative forces. These include irreversibilities due to mechanical losses, primarily from friction and sound energy, as well as thermal losses, including isentropic losses due to flow work caused by thermal fluid friction, heat leaks, and heat transfer losses (due to conduction, convection, and radiation).

Since the efficiency of every single Power Unit (PU) is less than 25% for air and less than 55% for helium as working fluids, some key factors for enhancing the efficiency of the SSPM structure must be developed and implemented. Therefore, the development and implementation of power systems characterized by generating more power than they consume for operation are absolutely disruptive in terms of thermal energy management and utilization. They fundamentally consist of a set of PUs connected in cascade, each equipped with special thermal energy management capabilities. This results in an SSPM. To achieve such a disruptive effect, a series of key constructive and operational factors must be met:

In summary, the essential key factors to achieve an SSPM require performing useful mechanical work by:

1. Expansion of a TWF due to a previous heat addition task under a closed isochoric process.

2. Contraction of a TWF due to a previous heat extraction task under a closed isochoric cooling process.

3. Work produced by the heat efficiently recovered from the counter-flow heat transfer cooling of the working fluid in the contraction processes of each upstream PU.

However, these essential factors must be accompanied by the following key strategies:

1. A unified heat carrier circuit for cascaded Power Units (PUs) responsible for both adding and recovering heat efficiently.

2. A high value of the RIT (Ratio of Initial isochoric Temperature to Final isochoric Temperature, $T_1/T_2$ or $T_1/T_{3)}$ to enhance the thermal efficiency of each individual PU while considering the importance of implementing the SSPM with the minimum number of PUs.

3. The task of supplying heat to the top PU in the cascade coupling structure is carried out using one of the available heat transfer techniques based on heat recovered overlay using the thermal energy superposition potential technique, which involves adding heat to the recovered working fluid by increasing the temperature of the recovered cooling fluid, approaching nearly 100% transfer effectiveness. This capability is due to the properties exhibited by electric-based heaters.

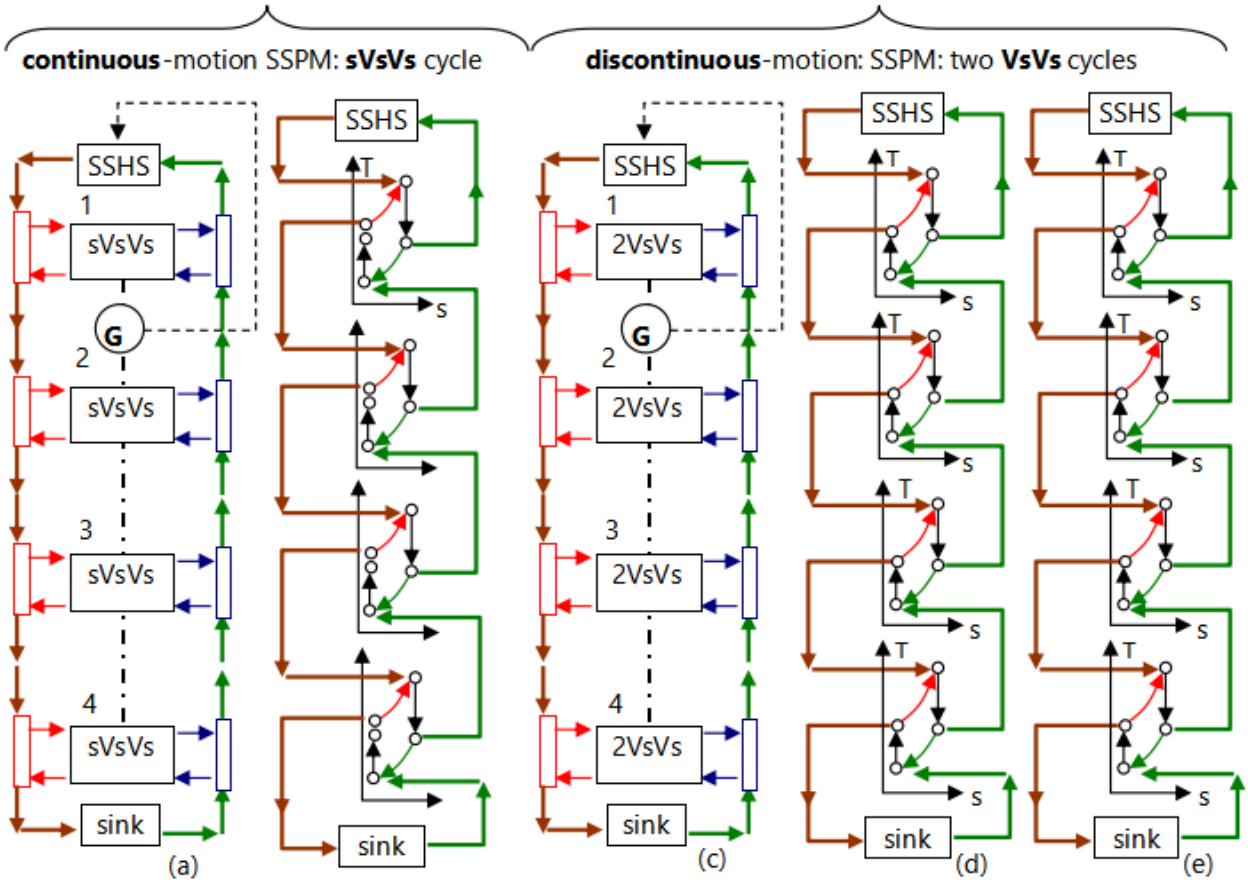


Figure 8: Flowchart of the closed circuit responsible for heat energy supply (brown) and heat energy recovery (green) of a SSPM.

This heat management strategy is illustrated in Fig. 8. Thus, in Fig.s 8(a) and (b) it is depicted the Heat Transfer Fluid (HTF) recirculation circuit used to feed thermal cycles of the sVsVs type whose thermal cycle diagram is depicted in Fig.(a) and (b). These cycles are characterized by their ability to provide useful mechanical work through thermal expansion, thermal contraction, and recovered heat from the cooling system of each upstream PU.

Fig. 8(a) depicts the SSPM implemented with cascaded PUs operating with the continuous motion sVsVs cycle depicted in Fig. 8(b). This cycle is characterized by exhibiting thermal working fluid reservoirs located outside the thermo-mechanical or thermo-hydraulic actuators. Fig. 8(c) depicts the SSPM implemented with cascaded PUs operating with the discontinuous motion VsVs cycle depicted in Fig.s 8(d) and (e). Both VsVs cycles are characterized by exhibiting thermal working fluid reservoirs located inside the thermomechanical or thermo-hydraulic actuators.

**4. 3 Case studies: Implementation an SSPM with PUs operating with sVsVs thermal cycle**

The basic scheme of a generic self-sustained thermal power plant equipped with the fundamental means to provide downstream heat to each PU coupled in cascade, as well as recover the cooling heat of each PU to be conducted upstream and feed back to the first PU (PU1) of the cascade, is represented in Fig. 9. The useful mechanical work produced by each PU is converted to electrical power, being managed in such a way that a fraction of the electrical power is returned to the heat addition system to the PU1, while the remaining electrical power is sent to the distribution network.

The fraction of electrical power sent to the PU1 is previously converted to heat by one of the available means: heating system based on electrical resistances, electro-inductive heating system or microwave heating system. Likewise, an alternative direct mechanical means of work-heat conversion through friction in a liquid could be used. The number of PUs in the plant is a function of two parameters: Temperature range available between the power source and the sink and the chosen value of the ratio ($T_1/T_2$), denoted as RIT for each PU.

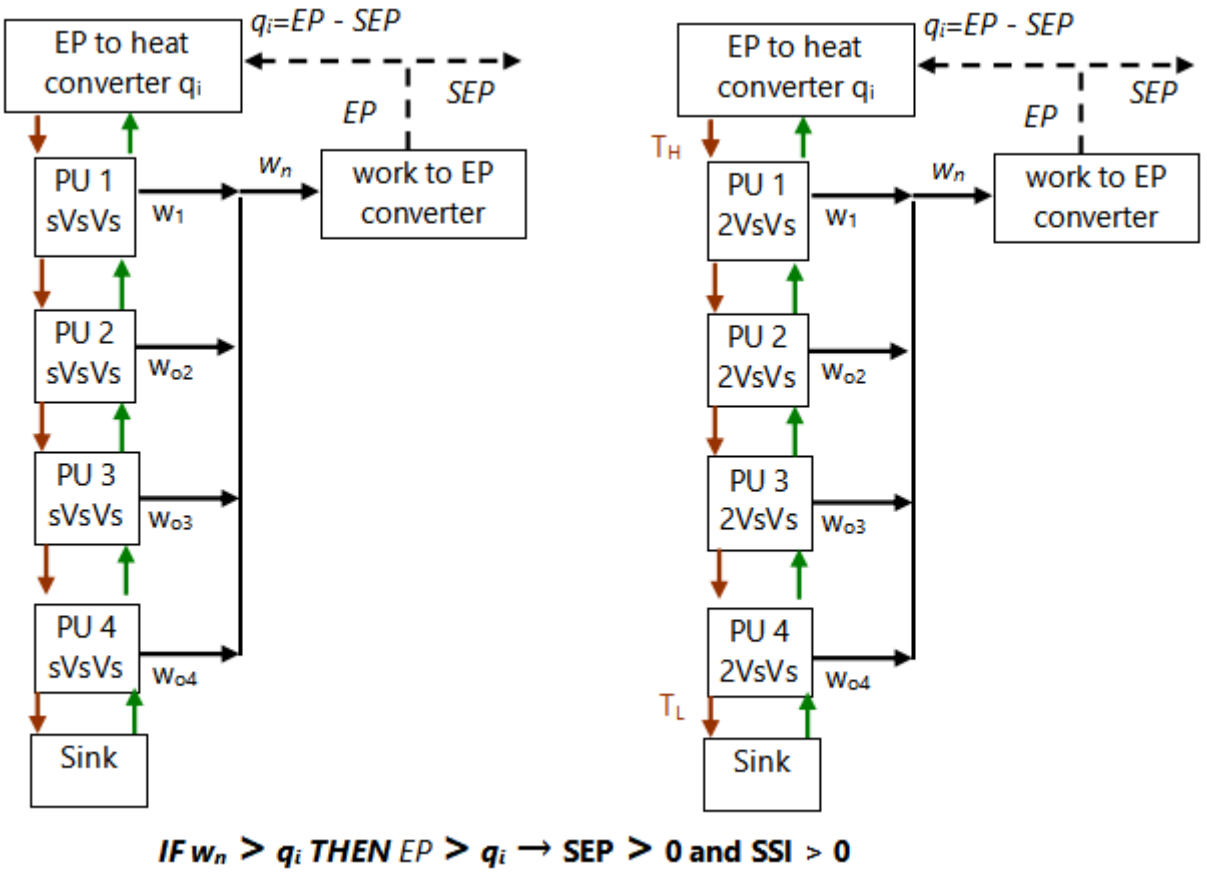


Figure 9: Schematic structure of a SSPM as the paradigm of a self-sustaining power machine (SSPM) showing the inlet temperatures of every PU downstream with a RIT = 0.85, as well as the temperatures of the recovered heat of PUs upstream. Acronyms used are: EP, electrical power; SEP, self-electrical power; EP-SEP, amount of heat to feed PU0.

According to the plant structure depicted in Fig. 9, energy balance is carried out according to the following model:

The total mechanical work is defined as,

$$w_n = \sum_{j=1,n} w_j \tag{34}$$

where the required amount of heat to feed the first PU of the cascade structure, is given as

$$q_{i(PU1)} = EP - SEP \tag{35}$$

Thus, the condition to achieve a feasible SSPM is written as,

$$IF\ w_n > q_{i(PU1)}\ THEN\ SEP > 0 \tag{36}$$

This means that output electric power (EP) is greater than the added heat energy $q_i$, so that there exist a free-cost useful energy available, that is, SEP. Such condition is represented as

$$IF\ w_n > q_{i(PU1)}\ THEN\ EP > q_{i(PU1)} \tag{37}$$

So, starting from this notable difference in behavior in terms of thermal efficiency between PUs that operate through expansion and contraction (case of the VsVs thermal cycle), it is about analyzing both cases and draw the pertinent conclusions. The structure of the analysis obeys the scheme shown in Fig. 10 using equations (18-21) to compare the final results of each SSPM.

Energy management in each SSPM is carried out in accordance with the flow diagram of energy manipulated in heat-work-electrical energy interactions shown in Fig. 10, such that the heat addition options can be electrical or mechanical: Among the electrical options we have heating techniques by electrical resistance, magnetic induction or microwave, while among the mechanical options we have friction in liquid fluids and drag in gaseous fluids, which is not considered in this work.

Finally, the self-sustained index (SSI) is used to establish the quality criterion of the net free energy delivered by the SSPM in terms of the amount in percentage of nominal design power of energy obtained at free cost:

$$SSI(\%) = \frac{\eta_{th} - 100}{100} \tag{38}$$

According Equation (38), if the global thermal efficiency satisfies the condition ($\eta_{th} < 100$) then, SSI is negative, indicating the amount of heat demanded from an external heat source to keep the engine active, which is a verification of the impossibility of a real perpetual motion machine of second kind.

**4.4 Case study: SSPM based on cascaded PUs equipped with the sVsVs cycle for air and helium as working fluids**

The study to be carried out on the SSPM with PUs implemented by means of thermo-hydraulic actuators concerns to the continuous-motion thermal cycle sVsVs. It studies a variety of thermal cycles characterized by closed processes that perform mechanical work both through the expansion and contraction of the TWF.

The sVsVs thermal cycle diagrams shown in Fig.s 4 (a) and (b) exhibit thermal contraction and therefore performs useful mechanical work by expanding and contracting the TWF. In this study, both individual and collective thermal efficiency is tested, that is, when it constitutes a thermal power plant formed by a group of sVsVs thermal cycles coupled in cascade in such a way that the cascade coupling structure composed by PUs ends when the heat exhausted by the last downstream cycle at its lowest temperature reaches a working temperature incapable to produce useful work. Likewise, the heat rejected by cooling each sVsVs thermal cycle is recovered upstream so that it can be reused through feedback to the first cycle of the cascade.

Table 3: sVsVs cycle data for air and helium as working fluids with RIT = 0.85

| sp | T(K) | p(bar) | V(m³/kg) | u(kJ/kg) | h(kJ/kg) | s(kJ/kg-K) | T(K) | p(bar) | V(m³/kg) | u(kJ/kg) | h(kJ/kg) | s(kJ/kg-K) |
|---|---|---|---|---|---|---|---|---|---|---|---|---|
| **PU1-Air** | | | | | | | **PU1-He** | | | | | |
| 1 | 680.00 | 2.00 | 0.6487 | 623.02 | 818.47 | 4.4153 | 680.00 | 2.00 | 4.6904 | 2124.00 | 3537.30 | 29.966 |
| 2 | 686.01 | 2.10 | 0.6334 | 627.72 | 826.05 | 4.4153 | 688.94 | 2.10 | 4.5994 | 2151.90 | 3588.97 | 29.966 |
| 3 | 800.00 | 2.62 | 0.6334 | 718.73 | 948.71 | 4.5380 | 800.00 | 2.60 | 4.5994 | 2498.00 | 4160.70 | 30.432 |
| 4 | 761.81 | 2.00 | 0.7267 | 687.91 | 913.15 | 4.5380 | 743.84 | 2.00 | 5.1304 | 2322.90 | 3898.08 | 30.432 |
| 5 | 652.00 | 1.57 | 0.7267 | 601.20 | 788.58 | 4.4153 | 640.00 | 1.58 | 5.1304 | 1999.40 | 3329.50 | 29.966 |
| **PU2-Air** | | | | | | | **PU2-He** | | | | | |
| 1 | 578.00 | 2.00 | 0.5513 | 544.33 | 764.17 | 4.2432 | 578.00 | 2.00 | 3.9873 | 1806.20 | 3272.50 | 29.122 |
| 2 | 583.19 | 2.10 | 0.5384 | 548.27 | 771.18 | 4.2432 | 585.59 | 2.10 | 3.9100 | 1829.80 | 3320.17 | 29.122 |
| 3 | 680.00 | 2.62 | 0.5384 | 622.98 | 883.17 | 4.3617 | 680.00 | 2.60 | 3.9100 | 2124.00 | 3849.10 | 29.588 |
| 4 | 646.71 | 2.00 | 0.6169 | 597.06 | 850.26 | 4.3617 | 632.26 | 2.00 | 4.3613 | 1975.30 | 3606.10 | 29.588 |
| 5 | 554.00 | 1.57 | 0.6169 | 526.21 | 736.72 | 4.2432 | 545.00 | 1.58 | 4.3613 | 1703.30 | 3080.20 | 29.122 |

| **PU3-Air** | | | | | | | **PU3-He** | | | | | |
|---|---|---|---|---|---|---|---|---|---|---|---|---|
| 1 | 491.30 | 2.00 | 0.4686 | 479.28 | 714.48 | 4.0746 | 491.30 | 2.00 | 3.3897 | 1536.00 | 3027.50 | 28.278 |
| 2 | 495.82 | 2.10 | 0.4577 | 482.62 | 720.90 | 4.0746 | 497.75 | 2.10 | 3.3239 | 1556.10 | 3071.50 | 28.278 |
| 3 | 578.00 | 2.62 | 0.4577 | 544.29 | 823.30 | 4.1896 | 578.00 | 2.60 | 3.3239 | 1806.20 | 3560.90 | 28.744 |
| 4 | 549.06 | 2.00 | 0.5237 | 522.44 | 792.86 | 4.1896 | 537.42 | 2.00 | 3.7076 | 1679.70 | 3335.99 | 28.744 |
| 5 | 470.50 | 1.57 | 0.5237 | 463.93 | 689.06 | 4.0746 | 463.00 | 1.58 | 3.7076 | 1447.80 | 2851.70 | 28.278 |
| **PU4-Air** | | | | | | | **PU4-He** | | | | | |
| 1 | 417.61 | 2.00 | 0.3982 | 425.07 | 668.95 | 3.9083 | 417.61 | 2.00 | 2.8817 | 1306.40 | 2800.90 | 27.434 |
| 2 | 421.49 | 2.10 | 0.3890 | 427.90 | 674.91 | 3.9083 | 423.09 | 2.10 | 2.8258 | 1323.50 | 2841.46 | 27.434 |
| 3 | 491.30 | 2.62 | 0.3890 | 479.22 | 768.57 | 4.0209 | 491.30 | 2.60 | 2.8258 | 1536.10 | 3294.30 | 27.900 |
| 4 | 466.29 | 2.00 | 0.4447 | 460.78 | 740.48 | 4.0209 | 456.80 | 2.00 | 3.1519 | 1428.50 | 3086.13 | 27.900 |
| 5 | 400.00 | 1.57 | 0.4447 | 412.30 | 644.94 | 3.9083 | 393.40 | 1.58 | 3.1519 | 1230.90 | 2638.30 | 27.434 |
| **PU5-Air** | | | | | | | **PU5 -He** | | | | | |
| 1 | 354.96 | 2.00 | 0.3383 | 379.56 | 627.19 | 3.7434 | 354.96 | 2.00 | 2.4499 | 1111.20 | 2591.30 | 26.590 |
| 2 | 358.29 | 2.10 | 0.3305 | 381.96 | 632.74 | 3.7434 | 359.62 | 2.10 | 2.4024 | 1125.70 | 2629.30 | 26.590 |
| 3 | 417.61 | 2.62 | 0.3305 | 425.00 | 718.51 | 3.8546 | 417.61 | 2.60 | 2.4024 | 1306.40 | 3047.70 | 27.056 |
| 4 | 396.13 | 2.00 | 0.3777 | 409.42 | 692.53 | 3.8546 | 388.28 | 2.00 | 2.6796 | 1215.00 | 2855.55 | 27.056 |
| 5 | 339.60 | 1.57 | 0.3777 | 368.53 | 605.80 | 3.7434 | 335.00 | 1.58 | 2.6796 | 1045.80 | 2441.50 | 26.590 |

The resulting thermal plants are shown in Fig.s 11, in which Fig. 11 (a) operates with air as the TWF, while Fig. 11 (b) operates with helium as the TWF. In this study, the results of both thermal work fluids are compared, where it is observed that air is still valid to produce more mechanical work than the heat demanded to function as a self-sustained plant, providing a valid SSI value with a RIT of 0.85. Similarly, when operating with helium, significantly higher results are obtained in terms of the SSI value for a RIT of 0.85.

The data resulting from processing the VsVs cycle states for air and helium at each PU are shown in Table 4 using real gas values obtained from the NIST database [14]. The data related to TWFs Lemmon E. W., et all, (2007), [29].

Table 4: Results of case studies with the data from Table 3 for the irreversible SSPM composed of ten cascaded PUs operating with air as a working fluid under the sVsVs cycle obeying to the scheme depicted in Fig. 11(a)

| | Helium | | | | | | Air | | | | | |
|---|---|---|---|---|---|---|---|---|---|---|---|---|
| PU | 1 | 2 | 3 | 4 | 5 | Total | 1 | 2 | 3 | 4 | 5 | Total |
| LF | 0.85 | 0.85 | 0.85 | 0.85 | 0.85 | 0.85 | 0.85 | 0.85 | 0.85 | 0.85 | 0.85 | 0.85 |
| RF | 0.95 | 0.95 | 0.95 | 0.95 | 0.95 | 0.95 | 0.95 | 0.95 | 0.95 | 0.95 | 0.95 | 0.95 |
| RIT*100 | 0.85 | 0.85 | 0.85 | 0.85 | 0.85 | | 0.85 | 0.85 | 0.85 | 0.85 | 0.85 | |
| T2 | 800.0 | 680.0 | 578.0 | 491.3 | 417.6 | | 800.0 | 680.0 | 578.0 | 491.3 | 417.6 | |

| | | | | | | | | | | | | |
|---|---|---|---|---|---|---|---|---|---|---|---|---|
| T1 | 680.0 | 578.0 | 491.3 | 417.6 | 354.9 | 504.3 | 680.0 | 578.0 | 491.3 | 417.6 | 354.9 | |
| qi_12/PU | 346.1 | 294.2 | 250.1 | 212.6 | 180.7 | 1283.7 | 91.01 | 74.71 | 61.67 | 51.32 | 43.04 | 321.7 |
| qo_34 | 323.5 | 272.00 | 231.9 | 197.6 | 169.2 | 1194.2 | 86.71 | 70.85 | 58.51 | 48.48 | 40.89 | 305.4 |
| q_recov | 323.5 | 272.0 | 231.9 | 197.6 | 169.2 | 964.3 | 86.7 | 70.85 | 58.5 | 48.5 | 40.9 | 246.6 |
| T_rec_mean | 711.9 | 605.1 | 514.3 | 437.2 | 371.6 | | 720.9 | 612.4 | 520.2 | 441.9 | 375.5 | |
| wn/PU | 181.2 | 147.09 | 121.6 | 100.1 | 81.91 | 631.97 | 33.59 | 27.31 | 22.48 | 18.18 | 14.95 | 116.5 |
| η_th/PU | 52.36 | 50.00 | 48.62 | 47.10 | 45.33 | | 36.91 | 36.56 | 36.46 | 35.43 | 34.75 | |
| η_th_SSPM | | | | | | 149.6 | | | | | | 126.0 |
| SSI | | | | | | **49.6** | | | | | | **26.0** |

In Fig. 10, the cascaded structure of the five (PUs) in each SSPM is depicted. The SSPM shown in Fig. 10(a) operates with air as the working fluid, while the SSPM depicted in Fig. 10(b) uses helium as the working fluid.

Table 4 presents data resulting from the sVsVs thermal cycle analysis for both air and helium as working fluids. The structure of Tables 5 and 6 aligns with the first column, where LF/PUi, RF/PUi, RIT*100/PUi, $T_3$/PUi [K], $T_2$/PUi [K] represent input variables. Additionally, the output variables—$q_{i12}$/PUi [kJ/kg], $q_{o34}$/PUi [kJ/kg], $q_{rec}$/PUi [kJ/kg], $T_{q\_rec}$/PUi [K], $w_n$/PUi [kJ/kg], $\eta_{th}$/PUi [%], $\eta_{th}$/plant [%], and SSI %/plant—are assumed as results.

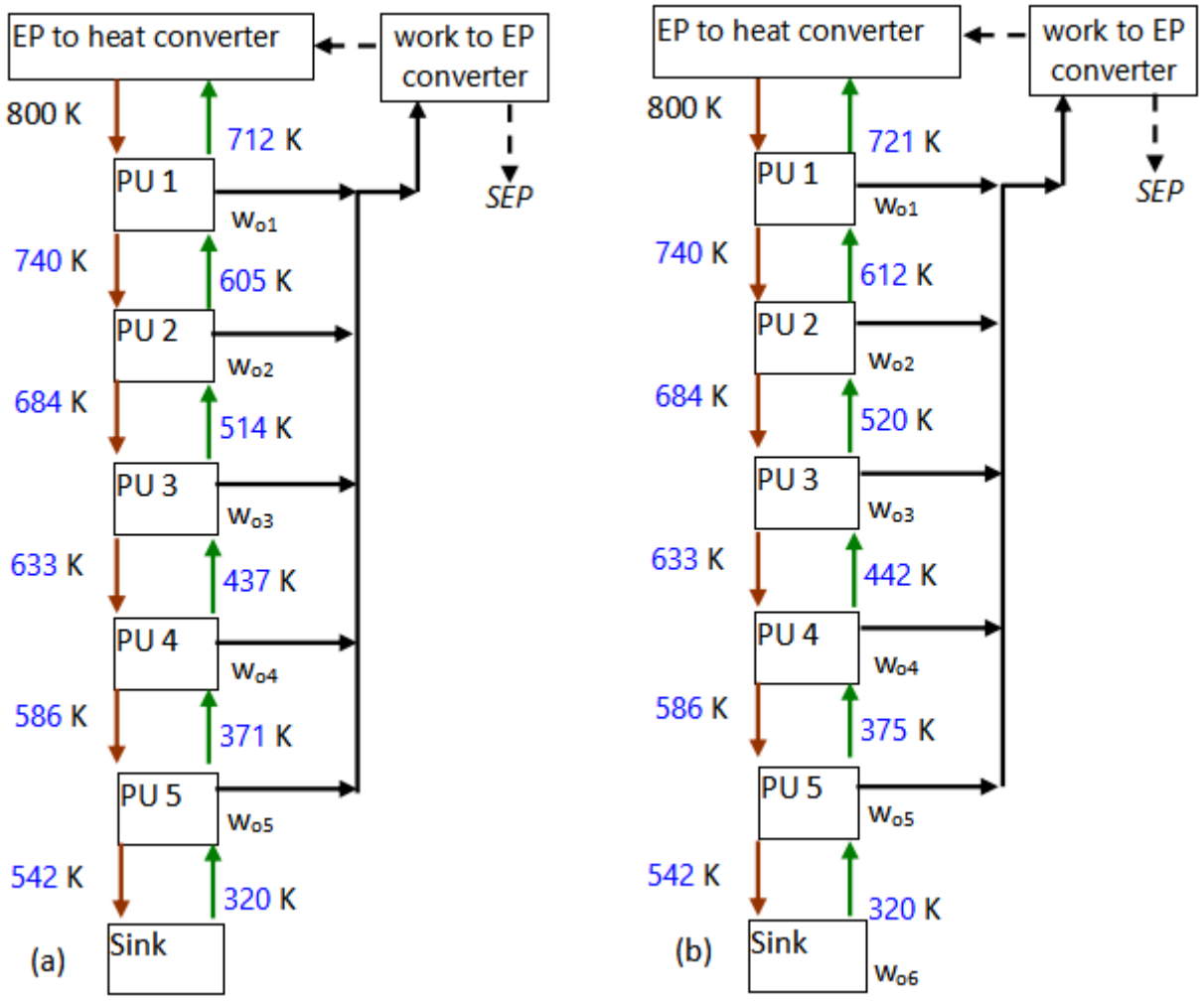

Figure 10: Case studies based on a sVsVs cycle according to Table 4: (a) SSPM operating with helium as working fluid. (b) SSPM operating with air working fluid

These results in Tables 4 and 6 allow us to assess the validity of the proposed input data based on the output results that best align with the expected performance of the implemented prototype. The energy balance, and consequent analysis is based on the first law and described by Equations (6)–(12), has been considered in this study.

The case study results, obtained from the data in Table 4, pertain to an irreversible SSPM composed of seven cascaded PUs operating with air and helium as working fluids under sVsVs cycles. These results focus on the SSPM's performance, particularly the SSI (Self-Sufficiency Index), as a function of the RIT (Recovered Input Temperature) considered being 0.85. The assumptions include a heat recovery factor (RF) of 0.85 and a losses factor (LF) of 0.85.

Table 5: VsVs cycle data for air and helium as working fluids with RIT = 0.85

| sp | T(K) | p(bar) | V($m^3$/kg) | u(kJ/kg) | s(kJ/kg-K ) | T(K) | p(bar) | V($m^3$/kg) | u(kJ/kg) | s(kJ/kg-K) |
|---|---|---|---|---|---|---|---|---|---|---|
| **PU1-Air** | | | | | | **PU1-He** | | | | |
| 1 | 680.00 | 1 | 0.97048 | 623.08 | 4.531 | 680.00 | 1 | 7.01880 | 2124.00 | 30.804 |
| 2 | 800.00 | 1.3555 | 0.97048 | 718.79 | 4.661 | 800.00 | 1.3553 | 7.01880 | 2497.90 | 31.310 |
| 3 | 766.60 | 1 | 1.09410 | 691.82 | 4.661 | 749.65 | 1 | 7.73740 | 2341.00 | 31.310 |
| 4 | 650.7 | 0.6954 | 1.09410 | 600.25 | 4.531 | 637 | 0.6975 | 7.73740 | 1990.00 | 30.804 |
| **PU2-Air** | | | | | | **PU2-He** | | | | |
| 1 | 578.00 | 1 | 0.82490 | 544.41 | 4.359 | 578.00 | 1 | 5.96650 | 1806.10 | 29.960 |
| 2 | 680.00 | 1.3556 | 0.82490 | 623.06 | 4.484 | 680.00 | 1.3552 | 5.96650 | 2124.00 | 30.466 |
| 3 | 650.86 | 1 | 0.92890 | 600.36 | 4.484 | 637.20 | 1 | 6.57720 | 1990.60 | 30.466 |
| 4 | 552.50 | 0.6955 | 0.92890 | 525.15 | 4.359 | 542.00 | 0.6992 | 6.57720 | 1693.90 | 29.960 |
| **PU3-Air** | | | | | | **PU3-He** | | | | |
| 1 | 491.30 | 1 | 0.7011 | 479.38 | 4.1906 | 491.30 | 1 | 5.0720 | 1536.00 | 29.116 |
| 2 | 578.00 | 1.3558 | 0.7011 | 544.39 | 4.3124 | 578.00 | 1.3552 | 5.0720 | 1806.20 | 29.622 |
| 3 | 552.69 | 1 | 0.7888 | 525.26 | 4.3124 | 541.62 | 1 | 5.5911 | 1692.80 | 29.622 |
| 4 | 469.30 | 0.6958 | 0.7888 | 463.14 | 4.1906 | 460.60 | 0.6989 | 5.5911 | 1440.30 | 29.116 |
| **PU4-Air** | | | | | | **PU4-He** | | | | |
| 1 | 417.61 | 1 | 0.59583 | 425.20 | 4.024 | 417.61 | 1 | 4.31170 | 1306.40 | 28.272 |
| 2 | 491.30 | 1.3560 | 0.59583 | 479.34 | 4.144 | 491.30 | 1.3552 | 4.31170 | 1536.00 | 28.778 |
| 3 | 469.39 | 1 | 0.66981 | 463.17 | 4.144 | 460.37 | 1 | 4.75290 | 1439.60 | 28.778 |
| 4 | 398.70 | 0.6963 | 0.66981 | 411.47 | 4.024 | 391.50 | 0.6988 | 4.75290 | 1225.00 | 28.272 |
| **PU5-Air** | | | | | | **PU5 -He** | | | | |
| 1 | 354.96 | 1 | 0.50626 | 379.72 | 3.860 | 354.96 | 1 | 3.66540 | 1111.10 | 27.428 |
| 2 | 417.61 | 1.3564 | 0.50626 | 425.16 | 3.978 | 417.61 | 1.3553 | 3.66540 | 1306.40 | 27.934 |
| 3 | 398.78 | 1 | 0.56893 | 411.49 | 3.978 | 391.31 | 1 | 4.04040 | 1224.40 | 27.934 |
| 4 | 338.70 | 0.69591 | 0.56893 | 368.03 | 3.860 | 354.96 | 1 | 3.66540 | 1111.10 | 27.428 |

Table 6: Results of case studies with the data from Table 5 for the irreversible SSPM composed of ten cascaded PUs operating with air as a working fluid under the **VsVs** cycle obeying to the scheme depicted in Fig. 11(a) for helium and 11(b) for air as working fluids.

| | Helium | Air |
|---|---|---|

| PU(i) | 1 | 2 | 3 | 4 | 5 | total | 1 | 2 | 3 | 4 | 5 | total |
|---|---|---|---|---|---|---|---|---|---|---|---|---|
| LF | 0.85 | 0.85 | 0.85 | 0.85 | 0.85 | | 0.85 | 0.85 | 0.85 | 0.85 | 0.85 | |
| RF | 0.95 | 0.95 | 0.95 | 0.95 | 00.95 | | 0.95 | 0.95 | 0.95 | 0.95 | 0.95 | |
| RIT*100 | 85.0 | 85.0 | 85.0 | 85.0 | 85.00 | | 85.0 | 85.0 | 85.0 | 85.0 | 85.00 | |
| T2 | 800.0 | 680.0 | 578.0 | 491.30 | 417.61 | | 800.00 | 680.00 | 578.00 | 491.30 | 417.61 | |
| T1 | 680.0 | 578.0 | 491.3 | 417.61 | 354.96 | | 680.00 | 578.00 | 491.30 | 417.61 | 354.96 | |
| qi_12/PU | 373.9 | 317.9 | 270.2 | 229.60 | 195.30 | 1386.90 | 95.71 | 78.65 | 65.01 | 54.14 | 45.44 | 338.95 |
| qo_34 | 351.0 | 296.7 | 252.5 | 214.60 | 182.60 | 1102.79 | 91.57 | 75.21 | 62.12 | 51.70 | 43.46 | 275.45 |
| q_recov | 298.3 | 252.2 | 214.6 | 182.41 | 155.21 | 937.37 | 77.83 | 63.93 | 52.80 | 43.95 | 36.94 | 234.13 |
| Tm_qrecov | 693.3 | 589.6 | 501.1 | 425.94 | 362.01 | | 708.65 | 601.68 | 511.00 | 434.05 | 368.74 | |
| wn | 222.5 | 187.88 | 159.96 | 136.02 | 115.74 | 822.15 | 38.10 | 32.10 | 27.06 | 22.87 | 19.40 | 139.53 |
| η_th | 59.52 | 59.10 | 59.20 | 59.24 | 59.26 | | 39.80 | 40.81 | 41.62 | 42.25 | 42.69 | |
| η_th_SSPM | | | | | | 182.89 | | | | | | 113.1 |
| SSI | | | | | | **82.89** | | | | | | **33.12** |

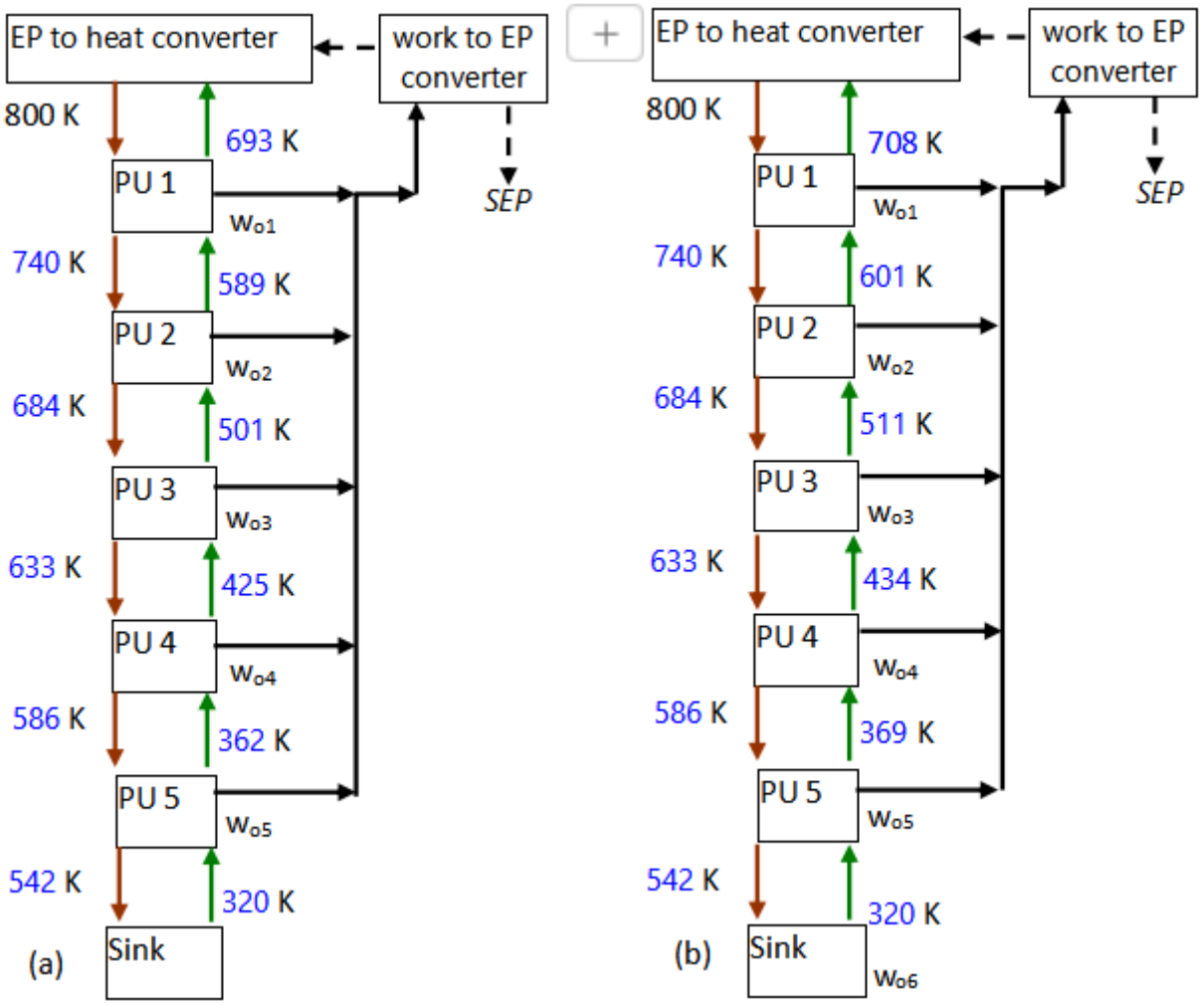


Figure 11: Case studies based on a **VsVs** cycle according to Table 6: (a) SSPM operating with helium as working fluid. (b) SSPM operating with air working fluid

**5 Analysis of results and discussion**

It is noteworthy that the thermal efficiencies among the sVsVs cycles remain nearly constant as the peak temperatures decrease, even when the thermal fluids are considered as real gases. This constancy is attributed to the temperature ratios (RIT = $T_1/T_3$) within each cycle adhering to the preselected value for the RIT, which is optionally chosen to be constant; in these case studies, the value is 0.85. In summary the thermal efficiencies are not influenced by the peak temperatures but rather by the temperature ratios. Thus, even with thermal fluids treated as real gases, the efficiencies remain almost constant.

Table 7: Comparison of the achieved global data resulting from tables 5 and 6 derived from case studies –air and helium respectively.

| Main results | sVsVs cycle | | VsVs cycle | |
|---|---|---|---|---|
| Number of PUs | 5 | 5 | 5 | 5 |
| Thermal fluid | Helium | Air | Helium | Air |
| LF | **0,85** | **0,85** | **0,85** | **0,85** |
| RF | **0.95** | **0.95** | **0.95** | **0.95** |
| RIT | **0,85** | **0,85** | **0,85** | **0,85** |

| | | | | |
|---|---|---|---|---|
| $\eta_{th}$/plant [%] | **149.6** | **126.0** | **183.0** | **133.0** |
| **SSI** [%]/plant | **49.6** | **26.0** | **83.0** | **33.0** |

Table 7 presents the comprehensive results for the two TWFs —air and helium— as real gases. Therefore, the most significant aspect of the global results for the thermal power plant utilizing sVsVs cycles, as shown in Table 7, is the SSI, which is defined previously. For a thermal power plant equipped with 5 PUs and using air as the TWF, the SSI value is **22.5**, corresponding to an efficiency of **122.5%**. In contrast, a thermal power plant with 5 PUs using helium as the TWF yields an SSI value of **84.0** equating to an efficiency of **184.0%**.

Consequently, based on the case studies object of the researched topic carried out in this section, which are focused on the fact that each PU, whose thermal cycle produces useful mechanical work through the thermal contraction of the TWF for sVsVs thermal cycles operating with helium, nearly increase four times the useful work output compared to air as TWF. Thus, the TWF is relevant to achieve the highest value of SSIs

As a result, a series of thermal cycles functioning through contraction can potentially increase significantly the total useful work output in comparison to the same plant structure o0erating with a non-convenient TWF.

Furthermore, if we consider the added benefit of recuperating the heat expended for cooling —which is responsible for the thermal contraction in each PU— and if this recovered heat is reintegrated into the power supply, it becomes apparent that the system can generate more useful work than the heat input required to power the first PU in the cascaded structure of PUs. Thus, recovery effectiveness is relevant to achieve the highest SSI

The overall results obtained with respect to the overall thermal efficiency shown in Tables 5 and 6 appear to represent a flagrant violation of the principle of energy conservation. However, all the Power Units (PUs) used in the implementation of the proposed power plants in both cases studied exhibit thermal efficiencies with values notably lower than 100% of the ideally possible efficiency.

Given the current scenario, how is it possible that with a group of PUs coupled in cascade, whose individual thermal efficiencies are much less than 100%, a global amount of useful work greater than the amount of heat required to power the single PU that needs external heat to ensure the operation of the power plant without additional heat requirements?. According to the average values of the thermal efficiency corresponding to the individual PUs that forms a SSPM observed in Tables 4 and 6, we have:

The relevant data summarized from Table 7 consists of the comparison of the achieved global data resulting from tables 5 and 6 derived from case studies operating with air and helium respectively.

Table 8: Summary of performance results

| Relevant data | sVsVs cycle | | VsVs cycle | |
|---|---|---|---|---|
| Thermal fluid | Helium | Air | Helium | Air |
| $\eta_{th}$/SSPM [%] | 149.6 | 126.0 | 183.0 | 133.0 |
| **SSI** [%]/SSPM | **49.6** | **26.0** | **83.0** | **33.0** |

Table 8 highlights the fact that the advantages of using sVsVs cycles versus VsVs cycles are evaluated in the following terms:

While PUs operating with the sVsVs cycle provide SSI values of 49.6 and 26% respectively for helium and air,

PUs operating with the VsVs cycle provide SSI values of 83 and 33% respectively for helium and air.

Although the SSI values are significantly lower for the sVsVs cycle compared to the VsVs cycle, the cost of each PU is significantly lower than that of the VsVs cycle, since the latter requires a double actuator structure for each PU to convert intermittent or discontinuous motion to continuous motion. In contrast, the need for external reservoirs for the sVsVs cycle increases the cost of each PU structure.

From the above data, some interesting facts can be deduced. Therefore, this means the SSPM using helium has nearly double the efficiency and self-sufficiency compared to using air. The key reasons are:

The thermal efficiencies of the individual PUs operating with helium are higher, ranging from 45-55%, compared to only 20-25% with air.

Helium has superior thermodynamic properties that allow it to extract more work from the heat addition and cooling processes in each PU.

In summary, the choice of working fluid has a major impact on the overall performance of the SSPM. Helium provides significantly better results than air, demonstrating the importance of fluid selection in maximizing the efficiency of this novel power generation concept.

The heat superposition capacity has a significant influence on the Self-Sufficiency Index (SSI) of the SSPM system:

**Key Findings:**

The ability to efficiently recover and reuse the heat expelled from the cooling of each upstream PU is a crucial factor in achieving a high SSI.

By recovering this heat and reintroducing it to power the first PU in the cascaded SSPM, the system can generate more useful work than the heat input required for the first PU.

This "heat superposition" strategy allows the SSPM to achieve thermal efficiencies greater than 100%, which would normally violate the laws of thermodynamics.

When using air as the working fluid, the SSPM with 5 cascaded PUs has an SSI of 22.5%.

In contrast, using helium as the working fluid increases the SSI to 84%.

The key reasons are:

- Helium has superior thermodynamic properties that allow it to extract more work from the heat addition and cooling processes in each PU.
- The recovered heat from the cooling of each upstream PU can be more effectively reused to power the first PU when using helium, leading to a higher SSI.
- The heat superposition strategy, where the recovered heat is reintegrated into the power supply, is a critical enabler for achieving SSI values greater than 100%.

In summary, the heat superposition capacity, enabled by the efficient recovery and reuse of cooling heat, is a crucial factor that allows the SSPM to achieve remarkably high SSI values, especially when using the superior working fluid of helium. This heat management strategy is a key innovation that sets the SSPM apart from traditional power generation systems.

The key relationship between thermal contraction and useful work output in the SSPM system is:

- Performing useful mechanical work through the thermal contraction of the working fluid, in addition to expansion, is critical for achieving high Self-Sufficiency Index (SSI) values.
- When the working fluid (TWF) undergoes thermal contraction in each PU, it generates significant additional useful work compared to expansion alone.
- For example, using helium as the TWF, the useful work output of the SSPM with 5 cascaded PUs operating under the sVsVs cycle increases significantly compared to using air, due to the superior contraction work.
- The ability to recover the heat expelled during the cooling process that drives the contraction, and reintegrate it to power the first PU, allows the system to generate more useful work than the initial heat input.
- This "heat superposition" strategy, enabled by the thermal contraction, is a key innovation that allows the SSPM to achieve thermal efficiencies greater than 100% and SSI values up to 184% with helium.

In summary, the thermal contraction of the working fluid is a crucial mechanism that enables the SSPM to extract significantly more useful work compared to traditional power cycles that rely only on expansion. Coupled with the efficient recovery and reuse of the contraction heat, it is a defining feature that allows the SSPM to achieve its remarkably high performance

It has been observed that the global efficiencies of the SSPM equipped with PUs operating with air as working fluid is about 33% less than the SSPM equipped with PUs operating with helium as working fluid. Therefore, the achievement of overall thermal efficiencies that exceed the ideally possible 100% limit value is not exclusively due to the upstream cascade heat recovery strategy but also to the contraction-based work. While the heat recovered in conventional power engines –without contraction work- consists mainly in low-grade heat, so that the opportunities to be efficiently reused as complement to the main power has been lost, as seen previously in this work, it is observed that the heat recovered has been upgraded by increasing its temperature or heat potential so that heat can be transferred to be efficiently reused. Such method concerns to infrared-based

electric heating technique by resistance heating or direct radiation, or by induction-based heating or by microwave radiation-based heating.

**5. Conclusions**

The article, "Prototyping disruptive self-sufficiency power machines composed by cascaded power units based on thermo-hydraulic actuators", presents a methodology to implement a SSPM that defies conventional laws of thermodynamics. As commented along the previous section, the selection of an appropriate Ratio of Isochoric Temperature is crucial for the design of both sVsVs and VsVs cycles in an SSPM that exhibit high SSI composed of cascaded PUs. That is, to achieve a high SSI, a higher RIT value allows more PUs to be cascaded, as it results in a narrower temperature range for each PU. This characteristic is important to maximize the thermal efficiency of the overall SSPM which means to maximize the SSI of the SSPM. The thermal efficiencies of the sVsVs and VsVs cycles remain nearly constant as the peak temperatures decrease, even when the working fluids (air and helium) are treated as real gases. The fact of obtaining an almost constant thermal efficiency in each PU with decreasing the peak temperatures of each cycle associated with each PU coupled in cascade is due to the contribution of the thermal contraction work obtained without energy cost. Consequently, an acceptable high SSI is attributed to the following factors:

-- the fact of taking advantage of the contraction-based work and

-- the value assumed for the RIT within each cycle adhering to the preselected constant value of 0.85.

-- acceptable rate of irreversibility due to the conversion of thermo-hydraulic energy to useful work which is assumed to be 0.85

The case study results presented in Tables 4 and 6 demonstrate the performance of an irreversible SSPM composed of 5 cascaded PUs operating with air and helium under the sVsVs and VsVs cycles, with a focus on the Self-Sufficiency Index (SSI) as a function of the RIT value of 0.85.

In summary, the key innovations consist of the utilization of thermal contraction to generate work, the specialized thermal cycles that leverage expansion and contraction, the efficient recovery and reuse of contraction heat, and the strategic selection of working fluids - all of which contribute to the SSPM's remarkable improvements in thermal efficiency and self-sufficiency.

To achieve such a level of improvements, some disruptive contributions have been carried out that gave rise to the following controversies with respect to the conventional statements:

Traditional exergy concept, first law (due to the energy balance of thermal cycles with contraction-based work), the energy balance of any SSPP, some aspects regarding to the second law, requires a deep revision to be adjusted according with observed experimental facts.

Therefore, since the article presents an intriguing theoretical framework that challenges our current understanding of thermodynamics, while the concepts proposed are highly controversial and appear to contradict well-established physical laws, the author acknowledge the need for an extensive experimental validation.

The proposed SSPM and its claimed ability to achieve efficiencies greater than 100% represent a significant departure from conventional thermodynamic principles. If successfully experimentally verified, such findings would have profound implications for our understanding of energy and power generation.

However, it's important to approach these claims with scientific scepticism. The extraordinary nature of the propositions demands equally extraordinary evidence. The call for prototyping and experimental validation is a crucial next step. Until such experiments are conducted and independently replicated, the scientific community is likely to remain sceptical of claims that appear to violate fundamental laws of thermodynamics. I am conscious of the situation that underscores the importance of the scientific method, where theoretical proposals must be subjected to rigorous experimental testing and peer review before they can be accepted as valid challenges to established scientific principles. Consequently, this approach acknowledges the potential significance of the claims while maintaining a cautious and scientifically sceptical stance, emphasizing the need for experimental validation.

I am therefore willing to cooperate with any research group who wishes to carry out a prototyping project, subject to an advantageously contract for the transfer of the patents property rights that we currently hold.

**References**


1. Wikipedia. Thomas Savery. https://en.wikipedia.org/wiki/Thomas_Savery
2. Wikipedia. Thomas Newcomen. https://en.wikipedia.org/wiki/Thomas_Newcomen
3. Wikipedia. James Watt: https://en.wikipedia.org/wiki/James_Watt; https://en.wikipedia.org/wiki/Watt_steam_engine
4. Müller. Gerald. The atmospheric steam engine as energy converter for low and medium temperature thermal energy. Renewable energy. 2013. vol. 53. p. 94-100. https://doi.org/10.1016/j.renene.2012.10.056
5. 5 Gerald Müller. George Parker. Experimental investigation of the atmospheric steam engine with forced expansion. Renewable Energy. Vol. 75. 2015. pp 348-355. ISSN 0960-1481. https://doi.org/10.1016/j.renene.2014.09.061.
6. Vítor Augusto Andreghetto Bortolin. Bernardo Luiz Harry Diniz Lemos. Rodrigo de Lima Amaral. Cesar Monzu Freire & Julio Romano Meneghini. Thermodynamical model of an atmospheric steam engine. Journal of the Brazilian Society of Mechanical Sciences and Engineering Vol. 43. 493 (2021). https://doi.org/10.1007/s40430-021-03209-9.
7. Ferreiro R. Ferreiro B. Isothermal and Adiabatic Expansion Based Trilateral Cycles. British Journal of Applied Science & Technology. 2015; (8) 5: 448-460. https://www.doi.org/10.9734/BJAST/2015/17350.
8. Ferreiro R. Ferreiro B. The Behavior of Some Working Fluids Applied on the Trilateral Cycles with Isothermal Controlled Expansion. British Journal of Applied Science & Technology. 2015; (9) 5: 694 450-463. https://www.doi.org/10.9734/BJAST/2015/18624.
9. Ramon Ferreiro Garcia. Jose Carbia Carril. Closed Processes Based Heat-Work Interactions Doing Useful Work by Adding and Releasing Heat. International Journal of Emerging Engineering Research and Technology. Volume 6. Issue 11. 2018. pp 8-23. ISSN 2349-4395 (Print) & ISSN 2349-4409 (Online). Accessed at: https://www.ijeert.org/papers/v6-i11/2.pdf; https://www.ijeert.org/v6-i11.
10. Ramon Ferreiro Garcia, Jose Carbia Carril, Manuel Romero Gomez and Javier Romero Gomez. Energy and entropy analysis of closed adiabatic expansion based trilateral cycles. Energy Conversion and Management 119 (2016) 49–59. http://dx.doi.org/10.1016/j.enconman.2016.04.031 .
11. Ramon Ferreiro Garcia. Reply to: Comment on ''Energy and entropy analysis of closed adiabatic expansion based trilateral cycles" by Garcia et al. Energy Conversion and Management 119 (2016) 49–59. Energy Conversion and Management 123 (2016) 646–648. http://dx.doi.org/10.1016/j.enconman.2016.06.05 .
12. Ramon Ferreio Garcia, Jose Carbia Carril. Combined Cycle Consisting of Closed Processes Based Cycle Powered by A Reversible Heat Pump that Exceed Carnot Factor. Journal of Advances in Physics, Volume 15, (2018), Pages: 6078-6100. ISSN: 2347-3487. DOI: 10.24297/jap.v15i0.8034.
13. Ramon Ferreiro Garcia. Study of the disruptive design of a thermal power plant implemented by several power units coupled in cascade. Energy Technol. 2023, 2300362 (1-17). Published by Wiley-VCH GmbH. DOI: https://doi.org/10.1002/ente.202300362
14. Ramón Ferreiro Garcia. Efficient disruptive power plant-based heat engines doing work by means of strictly isothermal closed processes. Journal of Advances in Physics Vol 22 (2024), p 30.53, ISSN: 2347-3487. https://rajpub.com/index.php/jap/article/view/9587. DOI: https://doi.org/10.24297/jap.v15i0.9587 .
15. Ramón Ferreiro Garcia. Design study of a disruptive self-powered power plant prototype. Journal of Advances in Physics Vol 22 (2024), p 62.92, ISSN: 2347-3487. https://rajpub.com/index.php/jap/article/view/9596. DOI: https://doi.org/10.24297/jap.v22i.9596 .
16. Ramón Ferreiro Garcia. Prototyping a Disruptive Self-Sustaining Power Plant enabled to overcome Perpetual Motion Machines. Journal of Advances in Physics Vol 22 (2024), p 141.178, ISSN: 2347-3487. https://rajpub.com/index.php/jap/article/view/963. DOI: https://doi.org/10.24297/jap.v22i.9633.
17. Ramón Ferreiro Garcia. Prototyping Self-Sustaining Power Machines with Cascaded Power Units Composed by Pulse Gas Turbines. Journal of Advances in Physics Vol 22 (2024), p 141.178, ISSN: 2347-3487. https://rajpub.com/index.php/jap/article/view/9648. DOI: https://doi.org/10.24297/jap.v22i.9648
18. E. W. Lemmon, M. L. Huber, M. O. McLinden, NIST Reference Fluid Thermodynamic and Transport Properties - REFPROP Version 8.0, User's Guide, NIST, Boulder, CO. 2007.
19. Patent: Planta térmica con máquina de doble efecto, acumuladores térmicos, convección forzada y alimentación térmica reforzada con un ciclo Brayton inverso y procedimiento de operación. Thermal power plant with double-effect machine, thermal accumulators, forced convection and reinforced thermal supply with a reverse Brayton cycle and operating procedure. Ramon Ferreiro Garcia, Jose Carbia Carril. application number 201700667 and publication number 2 696 950 B2. Accessed at: https://consultas2.oepm.es/ceo/jsp/busqueda/busqRapida.xhtml;jsessionid=m9dTemLOqYgGbpax1wR4K+aC.ConsultasC1
20. Patent: Procedimiento de operación de una máquina alternativa de doble efecto con adición y extracción de calor y convección forzada. Operating procedure of a double-acting reciprocating machine with heat

addition and extraction and forced convection and operating procedure. Jose Carbia Carril, Ramon Ferreiro Garcia, application number P201700718 and publication number 2 704 449 B2. Accessed at: consultas2.oepm.es/ceo/jsp/busqueda/busqRapida.xhtml;jsessionid=-wHy58sbfVYQutIYN8s0+JKK.ConsultasC1

21. Patent: Planta termoeléctrica multiestructural policíclica y procedimientos de operación. Polycyclic multi-structure thermal power plant and operating procedures. Ramon Ferreiro Garcia, application number P202200035 and publication number 2 956 342 B2. Accessed at: consultas2.oepm.es/ceo/jsp/busqueda/busqRapida.xhtml;jsessionid=-wHy58sbfVYQutIYN8s0+JKK.ConsultasC1